

Stochastic Geometry for Modeling, Analysis, and Design of Multi-Tier and Cognitive Cellular Wireless Networks: A Survey

Hesham ElSawy, Ekram Hossain, and Martin Haenggi

Abstract—For more than three decades, stochastic geometry has been used to model large-scale ad hoc wireless networks, and it has succeeded to develop tractable models to characterize and better understand the performance of these networks. Recently, stochastic geometry models have been shown to provide tractable yet accurate performance bounds for multi-tier and cognitive cellular wireless networks. Given the need for interference characterization in multi-tier cellular networks, stochastic geometry models provide high potential to simplify their modeling and provide insights into their design. Hence, a new research area dealing with the modeling and analysis of multi-tier and cognitive cellular wireless networks is increasingly attracting the attention of the research community. In this article, we present a comprehensive survey on the literature related to stochastic geometry models for single-tier as well as multi-tier and cognitive cellular wireless networks. A taxonomy based on the target network model, the point process used, and the performance evaluation technique is also presented. To conclude, we discuss the open research challenges and future research directions.

Index Terms—Multi-tier cellular networks, heterogeneous networks (HetNets), cognitive networks, interference modeling, stochastic geometry.

I. INTRODUCTION

DUE to the rapid proliferation of smart phones, tablets, and PDAs with powerful processing capability, the population of users using the wireless cellular infrastructure for Internet connectivity as well as the traffic demand per user are increasing dramatically. It is expected that by 2020 there will be more than 50 billion connected devices, and the cellular infrastructure should be developed accordingly [1]. The traditional homogeneous network expansion techniques via cell splitting cannot cope with the rapid growth of user population and their associated traffic. Moreover, macro base station (MBS) deployment necessitates a huge capital expenditure (CAPEX) which would be very difficult to recover with the decreasing service cost [2], [3]. In response to the capacity challenges, the industry is driving the standardization bodies to develop new solutions to accommodate the increased capacity

demand (i.e., network capacity and the link capacity)¹. For instance, small cells including femto cells have been added to the 3G, LTE and WiMAX standards, and many cellular service providers have already commercially launched their small cell services [3].

“Small cell” is an umbrella term for low-power and low-cost radio access nodes that operate in both licensed and unlicensed spectra and have a range of several meters to several hundred meters. Note that a typical mobile macrocell may have a range of up to several kilometers. The term “small cell” covers femtocells, picocells, microcells, and metrocells. When compared to unlicensed small cells (e.g., Wi-Fi), small cells operating in the licensed band (i.e., licensed small cells) provide support for legacy handsets, operator-managed quality of service (QoS), seamless continuity with the macro networks through better support for mobility/handoff, and improved security.

Some of the small cells (e.g., femto cells) are deployed and managed by the users, which means that some of the network CAPEX and operational expenditure (OPEX) are offloaded from the service providers to the users [3]. Small cells offer a fine grained and customer needs-oriented network expansion, which permits an optimized network operation. The small cells will offload a controllable percentage of the users and their associated traffic from the congested macro network tier, and hence, the number of users served by each network entity decreases, leading to a higher QoS per user. The network constituted by the MBSs overlaid by the small cell base stations (SBSs) is called a multi-tier cellular network (also referred to as a heterogeneous network [HetNet]). Multi-tier cellular network is a broad term that implies the coexistence of different networks (e.g., traditional macro cell as well as small cell networks) each of them constituting a network tier, and captures the single-tier (i.e., homogenous) cellular network as a special case. Multi-tier cellular networks are envisioned to provide a fast, flexible, cost-efficient and fine-tuned design and network expansion for the existing cellular architecture [2].

Due to the scarcity of the wireless spectrum along with the ever increasing capacity (both network and link capacities) demand, universal frequency reuse is one of the main characteristics of multi-tier cellular networks [3]–[7]. That is, the available spectrum will be aggressively reused by all of

Manuscript received February 13, 2013; revised April 24, 2013.

H. ElSawy and E. Hossain are with the Department of Electrical and Computer Engineering at University of Manitoba, Winnipeg, MB, Canada R3T 5V6 (e-mail: umelsawy@cc.umanitoba.ca, Ekram.Hossain@umanitoba.ca).

M. Haenggi is with the Department of Electrical Engineering at the University of Notre Dame, Indiana, USA (e-mail: mhaenggi@nd.edu).

Digital Object Identifier 10.1109/SURV.2013.052213.00000

¹Hereafter, we will use the term network capacity to refer to the total number of active users per unit area that can be accommodated by the network, and the link capacity to indicate the achievable data rate for a user using Shannon’s formula.

the coexisting network tiers. This will increase the spatial spectrum efficiency and network capacity at the expense of increased interference. In a multi-tier cellular network with universal frequency reuse and K coexisting tiers, there are two types of interferences, namely, the cross-tier (or inter-tier) interference and the co-tier (or intra-tier) interference. In the downlink, the cross-tier interference is the interference experienced by a user served by a BS from tier i from BSs belonging to tier j , $\forall j \neq i$, $j = 1, 2, 3, \dots, K$. On the other hand, the co-tier interference is the interference experienced by a user served by a BS in tier i from the other BSs in the same tier i . In multi-tier cellular networks, interference is one of the main performance limiting parameters, and hence, interference modeling, coordination, and avoidance are of primary interest to both the academic and industry communities. Cognitive (or intelligent) radio technology, which enables the radio devices to dynamically adjust the transmission parameters based on the ambient radio environment, will be an enabling technology for interference management and avoidance in multi-tier cellular networks [5].

For the analysis and design of interference avoidance and management techniques in multi-tier cellular networks, rigorous yet simple interference models are required. However, interference modeling has always been a challenging problem even in simple traditional single-tier cellular networks. For interference characterization, assuming that the BSs of the cellular network follow a regular grid (e.g., the traditional hexagonal grid model) leads to either intractable results which require massive Monte Carlo simulation [8] or inaccurate results due to unrealistic assumptions [9]. Moreover, due to the variation of the capacity (both network and link capacities) demand across the service area (e.g., downtowns, residential areas, parks, sub-urban and rural areas), the BSs will not exactly follow a grid-based model. That is, for snapshots of a cellular network at different locations, the positions of the BSs with respect to (w.r.t.) each other will have random patterns. Hence, the grid-based modeling assumption is violated and is considered too idealized. If topological randomness is a characteristic of the single-tier cellular networks, multi-tier cellular networks with independent deployment of small cells (e.g., femto cells) will have even more topological randomness.

Recently, a new modeling approach has been adopted for multi-tier cellular networks. It is based on stochastic geometry and not only captures the topological randomness in the network geometry but also leads to tractable analytical results. Stochastic geometry is a very powerful mathematical and statistical tool for the modeling, analysis, and design of wireless networks with random topologies [10]–[16]. It has been applied to ad hoc networks for more than three decades [17], in particular to model and analyze systems with random channel access (e.g., ALOHA [17]–[39] and carrier sensing multiple access (CSMA) [40]–[51]), single- and multi-tier cellular networks [52]–[80], and networks with cognitive elements [76]–[86].

In this article, we will not delve into the literature related to interference modeling in large-scale ad hoc networks because there exist excellent resources dealing with them [11]–[16]. Instead, we will focus on the related literature on stochastic geometry modeling and analysis of single-tier, multi-tier, and

cognitive cellular networks, which was not considered in [11]–[16]². Nevertheless, we will shed light on some stochastic geometric models for interference in large-scale ad hoc wireless networks which are necessary to give the mathematical preliminaries required to understand the discussion throughout this article. We will also provide a detailed taxonomy of the existing literature according to the point process used, the interference modeling approach, and the target network model. The proposed taxonomy will reveal the popularity and applicability of the different point processes (PPs) and modeling techniques. Finally, we will discuss the limitations of stochastic geometry modeling, potential methods to overcome some of these limitations, open research problems, and future research directions.

The rest of the paper is organized as follows. The mathematical preliminaries for stochastic geometry modeling are presented in Section II. In Section III, we classify the stochastic geometry modeling techniques used in the literature and provide a taxonomy of these techniques. In Section IV, the stochastic geometry modeling for multi-tier cellular networks is surveyed. Stochastic geometry modeling for cognitive networks is discussed in Section V. Section VI provides future directions for stochastic geometry modeling of cellular networks. Finally, we discuss the merits and limitations of stochastic geometry modeling in Section VII before concluding the paper in Section VIII.

II. PRELIMINARIES ON THE STOCHASTIC GEOMETRY MODELING OF WIRELESS NETWORKS

In this section, we provide some mathematical preliminaries on the stochastic geometry modeling to help understand the discussions presented later in this paper.

A. Signal-to-Interference-Plus-Noise Ratio (SINR) Model

In wireless communications, the signal power decays with the distance between the transmitter and the receiver according to the power law

$$P_r(y) = P_t(x)Ah_{xy} \|x - y\|^{-\eta} \quad (1)$$

where $x \in \mathbb{R}^d$ is the spatial location of a test transmitter, $P_t(x)$ is the transmit power indexed by the transmitter location, $y \in \mathbb{R}^d$ is the spatial location of the receiver, h_{xy} is a random variable accounting for the random channel (power) gain³ between the two locations x and y , $\|\cdot\|$ is the Euclidean norm, A is a propagation constant, and η is the path-loss exponent. Note that (1) is called the unbounded path-loss model due to its singularity at the origin. Although the unbounded path-loss model is only valid for calculating the received power at the far field, it has been extensively used in the literature due to its simplicity. An alternative path-loss model, called the bounded path-loss model, is more practical but complicates the analysis. The bounded path-loss model is given by

$$P_r(y) = \frac{P_t(x)Ah_{xy}}{\epsilon + \|x - y\|^\eta} \quad (2)$$

²The reason we focus on cognitive networks is that dynamic spectrum access via cognition is envisioned to be a key characteristic in a multi-tier network with self-organizing small cells [5].

³Random channel gains are used to model the uncertainties in the received signal power that arise due to multi-path fading and shadowing.

where $\epsilon > 0$ is added to avoid the singularity at the origin. While the choice of the model may significantly affect the interference statistics, its impact on the SINR statistics is smaller. More discussions on the effects of bounded and unbounded path-loss models can be found in [30]. Throughout this paper, for simplicity, we will use the unbounded path-loss model given in (1). Although (1) holds for any number of dimensions, the dimensions $d = 1, 2$, and 3 are of primary interest due to their physical interpretations.

Due to the distance-dependent signal power decay, along with the shared nature of the wireless medium, the network geometry has a significant impact on the performance of wireless networks. That is, the position of a test receiver w.r.t. its serving network entity highly affects the desired signal. On the other hand, the position of the test receiver w.r.t. other network entities that are simultaneously using the same channel highly affects the interference seen by the test receiver. Therefore, the network geometry has a significant impact on the SINR experienced by the receivers.

The SINR at a test receiver in the network can be calculated as

$$\text{SINR}(y) = \frac{P_t(x_0)Ah_{x_0y}\|x_0 - y\|^{-\eta}}{W + \sum_{x \in \mathcal{I}} P_t(x)Ah_{xy}\|x - y\|^{-\eta}} \quad (3)$$

where y is the location of the test receiver, x_0 is the location of the test transmitter (desired transmitter), $\mathcal{I} = \{x_1, x_2, \dots\}$ is the set of the locations of the interferers (active transmitters using the same channel as the test transmitter), and W is the noise power. The term $\sum_{x \in \mathcal{I}} \dots = I_{\text{agg}}$ is the aggregate interference power at the test receiver.

According to the network model, \mathcal{I} can be either finite or infinite, and the locations and the intensity of the interferers (i.e., the number of interferers per unit area) depend on the network characteristics (e.g., network topology, number of channels, association criterion, etc.) and medium access control (MAC) layer protocol (e.g., ALOHA, CSMA, TDMA, CDMA, etc.). The effect of user association and spectrum access method (i.e., MAC protocol) on the locations and/or intensities of the interferers are explained below.

- In a cellular network, a user may select the BS providing the highest signal power to be her serving BS. Therefore, in a single-tier cellular network, when all the BSs have the same transmit powers, the distance between a generic user and her nearest interfering BS will be greater than the distance between that user and her serving BS. In a multi tier cellular network, different network entities have different transmit powers. Therefore, as shown in Fig. 1(a), given that the distance between a macro-cell user and her serving MBS is r and the transmit power of the serving MBS is P_m , the nearest interfering MBS transmitting with the same power P_m will be located at a distance $r_m > r$. On the other hand, assuming the same path-loss exponent η for macro and small cell tiers, the nearest interfering SBS with transmit power P_s will be located at a distance $r_s > r \left(\frac{P_s}{P_m} \right)^{\frac{1}{\eta}}$. Similarly, Fig. 1(b) shows the relation between the desired link distance for a small cell user (i.e., the distance between the small cell user and her serving SBS) and the nearest interference sources.

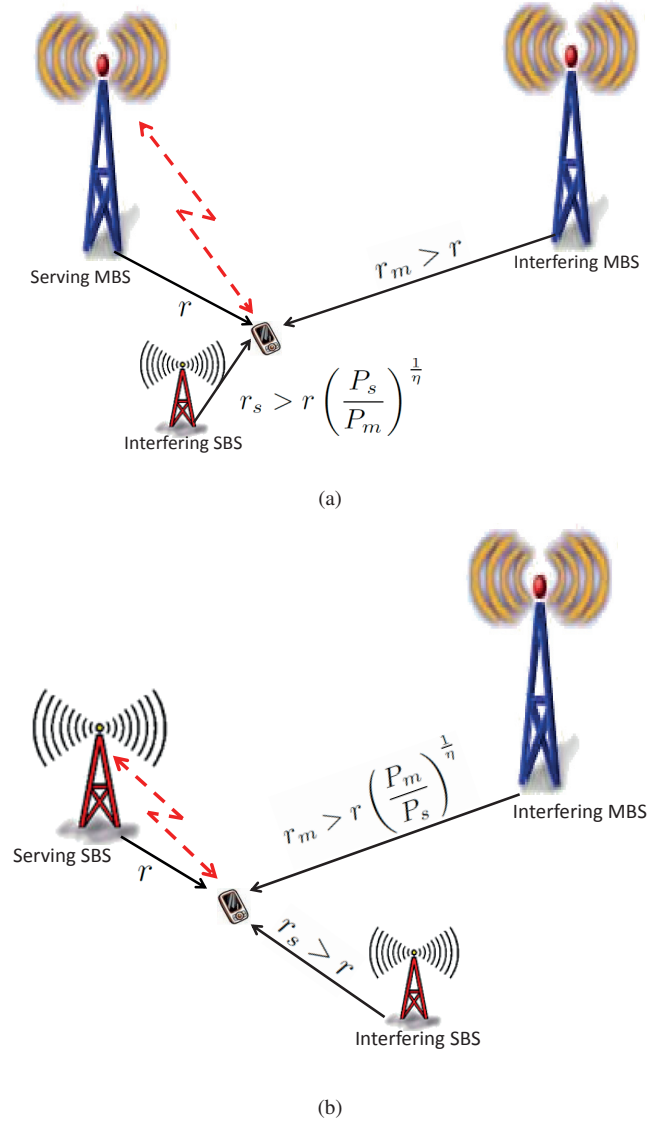


Fig. 1. The relation between the desired link distance and the nearest interference sources: (a) macro-cell user, (b) small-cell user.

- A cognitive spectrum access method affects both the locations of the interference sources as well as their intensity. In a cognitive cellular network, each network element performs spectrum sensing and accesses a channel if and only if the received power on that channel is less than a given threshold (γ). If deterministic channel gains are assumed, the spectrum sensing threshold (γ) translates to a minimum exclusion distance $r_e = \left(\frac{P_s A}{\gamma} \right)^{\frac{1}{\eta}}$ between the network elements using the same channel. Fig. 2(a) shows the locations of the cognitive network elements and Fig. 2(b) shows the potential locations of the simultaneously transmitting network elements on the same channel. From Fig. 2(b), we can see that there is a minimum distance between any two network elements using the same channel which controls both the minimum distance between a receiver and her interference sources as well as the intensity of the interference sources.

At a generic time instant, the SINR experienced by each receiver depends on its location, the positions of the inter-

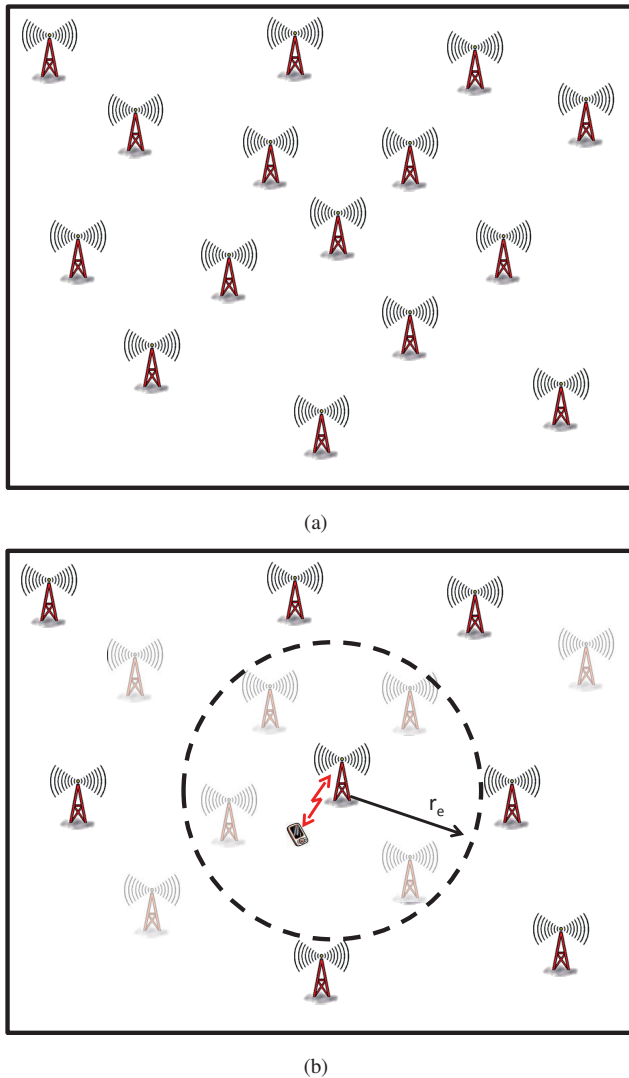


Fig. 2. (a) The locations of the cognitive network elements, (b) the potential locations of the simultaneously transmitting network elements on the same channel (the shaded network elements cannot simultaneously transmit on the same channel due to the cognitive nature of the spectrum access).

ference sources as well as the instantaneous channel gains. Hence, given the effect of network geometry on interference, the SINR is a random variable that strongly depends on the network geometry and significantly varies from one receiver to another and from one time instant to another.

Stochastic geometry is a mathematical tool that provides spatial averages, i.e., averages taken over large number of nodes at different locations or⁴ over many network realizations, for the quantities of interest (e.g., interference, SINR, outage probability, and achieved data rate) [11]. In other words, the stochastic geometry averages over all network topologies seen from a generic node weighted by their probability of occurrence [10], [83]. In this paper, after presenting the necessary preliminaries, we will elaborate how stochastic geometry captures the topological randomness while accounting for the system characteristics in cellular networks.

⁴If the point process is ergodic, the spatial averages (across points) equal the ensemble averages (across realizations) [10, Ch. 2].

B. Point Processes

In stochastic geometry analysis, the network is abstracted to a convenient point process (PP) which captures the network properties. That is, according to the network type, as well as the MAC layer behavior, a matching PP is selected to model the positions of the network entities. At first, we define the most popular PPs used in wireless communications systems, then we show the analogy between the PPs and the networks they model.

Definition 1 (Poisson point process (PPP)): A PP $\Pi = \{x_i; i = 1, 2, 3, \dots\} \subset \mathbb{R}^d$ is a PPP if and only if the number of points inside any compact set $\mathcal{B} \subset \mathbb{R}^d$ is a Poisson random variable, and the numbers of points in disjoint sets are independent.

Definition 2 (Binomial point process (BPP)): The BPP models the random patterns produced by a fixed number of points (N) in a set $\mathcal{B} \subset \mathbb{R}^d$ with a finite Lebesgue measure $L(\mathcal{B}) < \infty$, where $L(\cdot)$ denotes the Lebesgue measure⁵. Let $\Pi = \{x_i; i = 1, 2, 3, \dots\}$ and $\Pi \subset \mathcal{B}$, then Π is a BPP if the number of points inside a compact set $b \subseteq \mathcal{B}$ is a binomial random variable, and the numbers of points in disjoint sets are related via a multinomial distribution.

Definition 3 (Hard core point process (HCPP)): An HCPP is a repulsive point process where no two points of the process coexist with a separating distance less than a predefined hard core parameter r_h . A PP $\Pi = \{x_i; i = 1, 2, 3, \dots\} \subset \mathbb{R}^d$ is an HCPP if and only if $\|x_i - x_j\| \geq r_h, \forall x_i, x_j \in \Pi, i \neq j$, where $r_h \geq 0$ is a predefined hard core parameter.

Definition 4 (Poisson cluster process (PCP)): The PCP models the random patterns produced by random clusters. The Poisson cluster process is constructed from a parent PPP $\Pi = \{x_i; i = 1, 2, 3, \dots\}$ by replacing each point $x_i \in \Pi$ with a cluster of points $M_i, \forall x_i \in \Pi$, where the points in M_i are independently and identically distributed in the spatial domain.

More formal definitions of these PPs can be found in [10], [13], [14]. Fig. 3 shows a realization for a PPP and its corresponding HCPP and PCP. Note that every realization of a finite PPP is a BPP with the number of realized points [10, Thm. 2.9]. The PPP is used to model or abstract a network composed of a possibly infinite number of nodes randomly and independently coexisting in a finite or infinite service area [17], [18], [21], [25]–[28], [31] (e.g., nodes in a large-scale wireless network or users in a cellular network). If the total number of nodes is known and the service area is finite (e.g., a certain number of sensors dropped from a plane for battle field surveillance), then the BPP will be used to abstract the network [37], [38]. The PCP is used to model a network if the nodes are clustered according to certain social behavior or by the MAC protocol [39], [83] (e.g., users gathered around Wi-Fi hot spots). If there is a minimum distance separating the nodes due to some physical constrains (e.g., geographical constrains), due to network planning, or due to the MAC layer

⁵This is the standard way of assigning a measure to subsets of an n -dimensional Euclidean space. For $n = 1, 2, \text{ or } 3$, it coincides with the standard measure of length, area, or volume.

behavior, then a repulsive point process such as the Matérn HCPP will be used for modeling their spatial locations [40]–[51], [87], [88] (e.g., contention domain in a CSMA protocol).

The Matérn HCPP conditions on having a minimum distance r_h between any two points of the process, and is obtained by applying dependent thinning to a PPP. That is, starting from a PPP, the HCPP is obtained by assigning a random mark uniformly distributed in $[0, 1]$ to each point in the PPP, then deleting all points that coexist within a distance less than the hard core parameter r_h from another point with a lower mark. Hence, only the points that have the lowest mark within their r_h neighborhood distance are retained. As a result, no two points with a separation less than r_h will coexist in the constructed HCPP.⁶

Among these point processes, due to its independence property, the PPP is the most popular, most tractable, and most important. Models based on the PPP have been used for large-scale ad hoc networks for more than three decades [17], [18], [28], and the performance of PPP-based networks is well characterized and well understood. For instance, the exact probability density function (*pdf*) of the aggregate interference as well as the exact outage probability were obtained in [28] for a planar PPP network with deterministic channel gains and a path-loss exponent $\eta = 4$. Results for Rayleigh fading channels can be found in [19]. The exact distribution for the aggregate interference in a Rayleigh fading channel and a path-loss exponent $\eta = 4$ was derived in [29]. A model that captures general fading and propagation effects was developed in [31]. The maximization of transmission capacity⁷ was performed in [21], [26]. The exact upper and lower bounds on the outage probability can be found in [26]. The effect of fading channels and power control via channel inversion on the transmission capacity was studied in [20]. The effect of interference cancellation on the transmission capacity was studied in [22]. The transmission capacity-optimal decentralized power control policy for a PPP network was derived in [23], and the delay-optimal decentralized power control for PPP networks was derived in [33], [34]. The interference correlation due to mobility was characterized in [35]. Most of these results have been summarized in the two monographs [13], [14].

The importance of the PPP lies in that, besides being tractable and easy to handle, it does not only fit to model large-scale ad hoc networks with randomized multiple access techniques (e.g., ALOHA), it also provides tight bounds for the performance parameters in planned infrastructure-based networks and coordinated spectrum access networks. Moreover, as shown in the definitions above, the PPP provides the base line model (i.e., parent PP) for the different point processes used in the literature for wireless communications systems. For instance, in a coordinated access ad hoc network, the complete set of nodes attempting to access the spectrum can be modeled using a PPP. On the other hand, the subset of nodes selected by the MAC protocol to access the spectrum

⁶More precisely, this model is called a Matérn hard-core process of type II [10, Def. 3.8].

⁷The transmission capacity is a parameter that captures both the spatial frequency reuse efficiency and the outage probability. It is defined as the number of successful transmissions per unit area under an outage probability constraint [21].

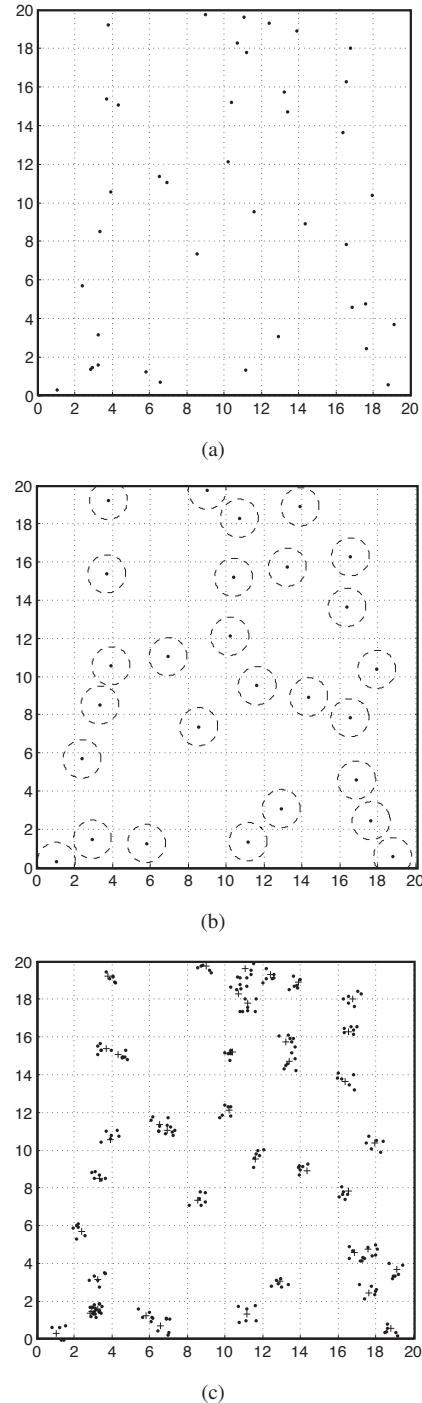


Fig. 3. (a) PPP in a $20\text{m} \times 20\text{m}$ region with intensity 0.1 points/ m^2 , (b) HCPP in a $20\text{m} \times 20\text{m}$ region for the parent PPP in (a) and hard core parameter $r_h = 2\text{m}$, each point of the HCPP lies at the center of a non-overlapping circles with radius $r_h/2$ represented by the dashed circles, (c) PCP in a $20\text{m} \times 20\text{m}$ region for the parent PPP in (a) and clusters with a Poisson distributed number of points with mean 2 uniformly distributed in a unit circle neighborhood (i.e., Matérn cluster process), the parent PPP points are plotted in crosses “+” while the added cluster points are plotted in dots.

will be modeled via the Matérn HCPP derived from the parent PPP modeling the complete set of nodes. Similarly, for an infrastructure-based network, a PPP can be used to model the set of candidate locations acquired by the site acquisition team for deployment of BSs, while a Matérn HCPP can be

used to model the subset of the locations selected by the network planning team for actual deployment of BSs. After abstracting the network by a convenient point process, several performance metrics can be characterized.

C. Performance Metrics

Interference is one of the main network parameters to characterize using the stochastic geometry analysis. For a generic node in the network, the aggregate interference $I_{\text{agg}} = \sum_{x \in \mathcal{I}} P_t(x) A h_{xy} \|x - y\|^{-\eta}$ is a stochastic process that depends on the locations of the interferers captured by the point process $\mathcal{I} = \{x_i\}$ and the random channel gains h_{xy} . Note that \mathcal{I} is defined by the network properties and the MAC layer as shown in Fig. 1 and Fig. 2. The aggregate interference is a stochastic process which varies according to the test location and time. As mentioned before, stochastic geometry analysis gives the statistics of the interference (averaged w.r.t. the spatial domain) behavior experienced by the nodes existing in the network. Hence, interference can be completely characterized by its *pdf* (or equivalently, its cumulative distribution function (*cdf*)). Generally, there is no known expression for the *pdf* of the aggregate interference in large-scale networks. Hence, the aggregate interference is usually characterized by using the Laplace transform (LT) of the *pdf* (or equivalently its characteristic function [CF] or moment generation function [MGF])⁸. The Laplace transform of the aggregate interference is given by

$$\mathcal{L}_{I_{\text{agg}}}(s) = \mathbb{E}[e^{-sI_{\text{agg}}}], \quad (4)$$

At a generic time instant, since the aggregate interference is a strictly positive random variable, its Laplace transform always exists. Stochastic geometry provides a systematic way to obtain the LT, CF, or MGF for the aggregate interference associated with the PP of interest. In this article, we will not go into the details of how to derive the LT, CF, or MGF for the aggregate interference associated with the PP of interest as they are well explained in the literature [11], [13], [14], [25], [27]. However, it is important to note that although the exact LT, CF, or MGF are available for the PPP, BPP, and the PCP, only approximate expressions of LT, CF, or MGF are available for the Matérn HCPP. With the LT, CF, or MGF, we are able to generate the moments (if they exist) of the aggregate interference as $\mathbb{E}[I_{\text{agg}}^n] = (-1)^n \mathcal{L}_{I_{\text{agg}}}^{(n)}(s) \Big|_{s=0}$, where $\mathcal{L}_{I_{\text{agg}}}^{(n)}(s)$ is the n^{th} derivative of $\mathcal{L}_{I_{\text{agg}}}(s)$. In the general case, it is not possible to derive the exact performance metrics (e.g., outage probability, transmission capacity, average achievable rate) from the LT, CF, or the MGF.

In the next section, we will show different techniques used in the literature to utilize the LT, CF, or the MGF and go beyond the moments of the aggregate interference to evaluate the network performance.

III. TECHNIQUES TO ANALYZE NETWORK PERFORMANCE

In the literature, there are five main techniques to utilize the LT, CF, or the MGF and go beyond the moments of

interference and model the network performance metrics. In the following, we will discuss the techniques which were used in the literature to overcome the obstacle imposed by the non-existence of any useful closed-form expression for the *pdf* of the interference.

A. Technique #1: Resort to the Rayleigh Fading Assumption

Because of its analytical tractability, the Rayleigh fading assumption is the most popular assumption in the literature to overcome the obstacle imposed by the non-existence of any closed-form expression for the *pdf* of the aggregate interference [25], [27]. Although the interference statistics cannot be obtained, by assuming Rayleigh fading on the desired link (i.e., the link between the test receiver and its serving transmitter), the exact distribution for the SINR can be obtained. That is, if the desired link is impaired by Rayleigh fading, the expression for the *cdf* of the SINR can be obtained from the Laplace transform evaluated at some value.

Without loss of generality, let $r = \|x_0 - y\|$ be the constant distance between the transmitter and the test receiver, $h_0 \sim \exp(\mu)$ be the channel power gain of the desired link, then we have

$$\begin{aligned} F_{\text{SINR}}(\theta) &= \mathbb{P}\{\text{SINR} \leq \theta\} \\ &= \mathbb{P}\left\{\frac{P_t A h_0 r^{-\eta}}{W + I_{\text{agg}}} \leq \theta\right\} \\ &= \mathbb{P}\left\{h_0 \leq \frac{(W + I_{\text{agg}})\theta r^\eta}{P_t A}\right\} \\ &= \int_u F_{h_0}\left(\frac{(W + u)\theta r^\eta}{P_t A}\right) f_{I_{\text{agg}}}(u) du \\ &\stackrel{(i)}{=} 1 - \mathbb{E}_{I_{\text{agg}}}\left[\exp\left(-\frac{(W + I_{\text{agg}})\mu\theta r^\eta}{P_t A}\right)\right] \\ &= 1 - \exp\left(-\frac{W\mu\theta r^\eta}{P_t A}\right) \mathbb{E}_{I_{\text{agg}}}\left[\exp\left(-\frac{I_{\text{agg}}\mu\theta r^\eta}{P_t A}\right)\right] \\ &= 1 - \exp\left(-\frac{W\mu\theta r^\eta}{P_t A}\right) \mathcal{L}_{I_{\text{agg}}}(s) \Big|_{s=\frac{\mu\theta r^\eta}{P_t A}} \\ &= 1 - \exp(-Wc\theta) \mathcal{L}_{I_{\text{agg}}}(s) \Big|_{s=c\theta} \end{aligned} \quad (5)$$

where $F_{h_0}(\cdot)$ is the *cdf* of h_0 , $f_{I_{\text{agg}}}(\cdot)$ is the *pdf* of the aggregate interference, the expectation in (i) is w.r.t. both the point process and the channel gains between the interference sources and the test receiver, and $c = \frac{\mu r^\eta}{P_t A}$ is a constant. Relaxing the constant distance r is straightforward [54]. As mentioned before, the LT for the aggregate interference can be found in a systematic manner [13]–[16]. For interference-limited networks (i.e., $I_{\text{agg}} \gg W$), the effect of noise can be ignored and the *cdf* reduces to $F_{\text{SINR}}(\theta) = 1 - \mathcal{L}_{I_{\text{agg}}}(s) \Big|_{s=c\theta}$, in which the Laplace transform of the aggregate interference is evaluated at some constant c multiplied by the parameter θ of the *cdf* of SINR. With the exact *cdf* of the SINR, different performance metrics such as the outage probability, transmission capacity, and the achievable data rate (i.e., obtained using Shannon's formula) can be quantified. This technique is used in [9], [25]–[27], [32]–[35], [37], [39], [54]–[60], [62]–[66], [68], [77], [78], [80], [81], [83], [85], [86], [89], [90].

The main drawback of this technique is that it is only valid with the Rayleigh fading assumption for the desired link,

⁸Hereafter, we will say “the Laplace transform of the random variable” to denote the Laplace transform of its *pdf*.

which may not always be the case. We can relax the Rayleigh fading assumption at the expense of the tractability of the model. As a result, we may be able to get only approximate solutions or tight bound on the SINR distribution.

B. *Technique #2: Resort to Dominant Interferers by Region Bounds or Nearest n Interferers*

Technique #2 is also a very popular technique because of its simplicity and accuracy. This is based on the idea of obtaining a lower bound on the outage probability by only considering the subset of dominant interferers. In the literature, it has been shown that, under a high path-loss exponent (e.g., $\eta = 4$), both the approaches (i.e., approaches based on the vulnerability region and nearest n interferers) give tight lower bounds on the outage probability. However, when the path-loss exponent decreases and approaches 2 (in the planar case), the contribution of distant interferers to the outage events increases and becomes overwhelming, and hence, both approaches lose their accuracy and therefore should not be used.

Assuming deterministic channel gains, the region bound is determined by the vulnerability circle around the test receiver. The vulnerability circle is the region where the signal power of any active transmitter measured at the test receiver is greater than the desired signal power at the test receiver multiplied by a certain threshold θ [12]. In other words, for a given SINR threshold θ , the vulnerability circle contains all transmitters where the transmission of any of them can alone corrupt the signal received at the test receiver. The notion of the vulnerability circle can be extended to random channel gains as in [77].

In the vulnerability region analysis, it is not required to derive the Laplace transform of the aggregate interference. Instead, only the spatial statistics of the PP are studied over the vulnerability region corresponding to the desired signal strength and the SINR threshold. That is, the outage probability (i.e., the *cdf* of the SINR) can be lower bounded by the probability that the vulnerability region is non-empty.

The approach based on the nearest n interferers leads to the same results (i.e., lower bounds), however, since the distribution of the distances for the n nearest interference sources needs to be determined, the analysis here is significantly more involved than the vulnerability region analysis. The distribution of distances for the PPP and BPP was derived in [36] and [38] respectively.

Since the moments of the aggregate interference can be generated from the LT, CF, or the MGF, an upper bound for the outage probability can be obtained using the Markov inequality, Chebyshev's inequality, or the Chernoff bound. The Markov inequality is the easiest to compute, however, it is the most loose inequality. On the other hand, the Chernoff bound is quite tight for the tail probability, but its computation is more involved and requires the knowledge of the MGF to be optimized. Generally, the lower bounds provided by the region bounds or the n nearest interferers are tighter than these upper bounds [26]. The lower bound obtained based on the vulnerability region analysis was used in [17], [18], [21]–[26], [39], [43]–[45], [67], [69]. The bound based on the

nearest n interferers was used in [19], [20], [35], [38], [81]. The Markov upper bound was used in [22], [25], [26], [39]. The Chebyshev's upper bound was used in [20]–[22], [26], [43], [69] and the Chernoff upper bound was used in [26].

C. *Technique #3: Resort to the Approximation of the pdf of the Aggregate Interference*

In technique #3, the *pdf* of the aggregate interference power is approximated by one of the known *pdfs*. The parameters of the approximate *pdf* are obtained via the LT, CF, or MGF. For instance, if the *pdf* of the aggregate interference is approximated by a normal distribution, then the mean and the standard deviation will be obtained from LT, CF, or the MGF of the aggregate interference. The main drawback of this method is that there is no known criterion to choose which *pdf* to use and the approximation error can be only quantified by simulations.

In the literature, different papers used different *pdfs* according to the problem in hand and the results were verified via simulations. For a PPP, it was discussed in [25], [27] that under the bounded path-loss or a guard zone around the receiver, the moments of aggregate interference exist and the distribution of it approaches the Gaussian distribution. In [37], [43], [46], the aggregate interference was approximated via a Gaussian distribution. However, in [82] it was shown that the *pdf* of aggregate interference from a PPP with an exclusion region around the test receiver is skewed and hence deviates from normality. The authors in [82] showed that the shifted log-normal distribution gives a better approximation than the Gaussian approximation for the *pdf* of the secondary users' aggregate interference in a cognitive network. In [84], the *pdf* of aggregate interference power was approximated by a truncated stable distribution, and in [76] by log-normal and shifted log-normal distributions. In [13, Sec. 5.5], the gamma, inverse Gaussian, and the inverse gamma distributions were used to model interference powers under general PPs. In [71], the *pdf* of the amplitude of the aggregate interference was approximated with a circularly symmetric complex Gaussian distribution.

D. *Technique #4: Resort to the Plancherel-Parseval Theorem*

The Plancherel-Parseval theorem [91] states that if $f_1(t)$ and $f_2(t)$ are square integrable complex functions, then

$$\int_{\mathbb{R}} f_1(t)f_2^*(t)dt = \int_{\mathbb{R}} \mathcal{F}_1(\omega)\mathcal{F}_2^*(\omega)d\omega \quad (6)$$

where $\mathcal{F}_1(\omega)$ is the Fourier transform (FT) of $f_1(t)$, $\mathcal{F}_2(\omega)$ is the FT of $f_2(t)$, and $f^*(t)$ denotes the conjugate of $f(t)$. The Fourier transform of a *pdf* is equivalent to the CF of that *pdf*, which is a special case of the Laplace transform and is obtained as $\mathcal{F}(\omega) = \mathcal{L}(s)|_{s=i\omega}$, where $i = \sqrt{-1}$. The Plancherel-Parseval theorem precludes the need of inverting the Laplace transform (i.e., obtaining the *pdf* of the interference) obtained from the stochastic geometry analysis to obtain the performance metrics. Moreover, with the aid of the Plancherel-Parseval theorem, results for general fading environment can be obtained by stochastic geometry analysis. However, the main drawback here is that the integrals are

quite involved due to the complex nature of the characteristic functions. Hence, the stochastic geometry analysis loses its main merit which is the analytical tractability that leads to simple closed-form equations, and in turn, helps understanding the behavior of the tested system in response to variations in the design variables. Nevertheless, the Plancherel-Parseval theorem provides a mathematically elegant technique to extend all of the existing stochastic geometry results for general fading environments. It was used in [15], [16], [32], [42].

E. Technique #5: Inversion

In this technique, the LT, CF, or MGF is inverted to obtain the *pdf* of the interference [28]–[31], [40], [41], [70], [71]. Due to the complex nature of the expressions for the LT, CF, or MGF, generally we cannot find the *pdf* in closed form. This technique is only useful for very special cases of the PPP where the expressions for LT, CF, or MGF are invertible or match the LT, CF, or MGF of a known distribution [28], [29], [31], [70], [71]; otherwise, inversion is done numerically [30], [40], [41]. For instance, the Laplace transform of the aggregate interference, measured at a receiver located at an arbitrary origin in \mathbb{R}^d , associated with an infinite PPP that starts from that arbitrary origin (i.e., there is no interference protection region around the receiver defined by the MAC layer) with unbounded path-loss function (e.g., eq. (1)) matches the Laplace transform of an alpha-stable distribution⁹ [11]–[14]. Although this result looks promising, it is not very useful because the unbounded path-loss results in a significant deviation from reality due to the singularity at the origin [30]. Hence, the interference does not have finite moments. Moreover, dealing with alpha-stable distributions is tricky since they do not provide a closed-form expression for the *pdf*. The only two exceptions where the *pdf* of interference has a closed-form expression can be found in [28] for deterministic channels, and in [29] for Rayleigh fading channels. Both the closed-form *pdf*s were obtained under the assumptions of an unbounded path-loss model, an infinite PPP, and path-loss exponent $\eta = 4$.

F. Summary and Taxonomy

Fig. 4 and Table I provide a taxonomy for the literature according to the target network model, the point process used, and the technique to utilize the LT, CF, or the MGF for performance evaluation. Note that if the same reference appears in different categories of the taxonomy, this means that this reference uses all of these techniques. The taxonomy clearly shows the popularity of each point process and each performance modeling technique. From Fig. 4 and Table I we can see that the PPP is the most popular point process used in the literature because of its simplicity. Furthermore, the PPP provides accurate performance bounds and it is the parent point process for the HCPP and the PCP. The HCPP has also been extensively used to model wireless communication systems due to the hard core condition (i.e., the minimum distance r_h) which captures the contention-based spectrum access [40]–[51]. Furthermore, in [92], the authors showed

that, compared to the PPP, the HCPP better captures the spatial distribution of the base stations in a real network deployment.

To summarize, in stochastic geometry modeling we use point processes (PPs) to model the locations of the network entities. Then, the LT, CF, or the MGF of the aggregate interference is obtained. In this article, we have not shown how to obtain the LT, CF, or the MGF of the aggregate interference associated with the PP of interest because it is generally straightforward and is available in [11], [13]–[16]. Finally, according to the accuracy, tractability, and practicality tradeoffs, one of the five techniques in the literature as discussed above is chosen to derive the performance metrics of interest from the LT, CF, or the MGF of the aggregate interference. Some examples that show when to use each of the five performance evaluation techniques are provided below.

- For a network with general fading in the interference links and Rayleigh fading in the desired link, technique #1 is the right technique to use. As shown in Fig. 4 and Table I, technique #1 has been extensively used in the literature because it is simple and gives the exact distribution for the SINR.
- If general fading is observed on the desired link, then a lower bound via technique #2 can be obtained. It is worth mentioning that the lower bound in technique #2 is generally tighter than the upper bounds [26]. Note that the accuracy of the lower bound increases for higher values of the path-loss exponent due to the faster signal decay which makes the effect of far interferers negligible.
- On the other hand, for lower values of the path-loss exponent, it is better to use technique #3 and have an approximate analysis. It has been shown that for the approximation of the *pdf* of interference, the shifted log-normal distribution is better than both the Gaussian and log-normal distributions [76], [82]. However, there is no known method to validate the approximation except by simulations.
- With general fading in the direct (i.e., desired) link, if an exact analysis is required, then technique #4 has to be used, but the analysis will be highly involved. From Fig. 4 and Table I it can be observed that technique #4 has not been frequently used in the literature due to its analytical complexity.
- Finally, technique #5 is only limited to some special cases as far as only the analytical evaluation is concerned.

In the next section, we will not go into the mathematical details used in the references which deal with stochastic geometry modeling of wireless networks. However, for each reference we will clearly show how to reduce the problem at hand into one of the known PPs and which technique out of the popular five techniques is used for performance evaluation.

IV. STOCHASTIC GEOMETRY MODELING APPROACHES FOR MULTI-TIER CELLULAR NETWORKS

Multi-tier cellular networks consist of macro BSs (MBSs) overlaid by different tiers of small cells (i.e., micro BSs (MiBSs), pico BSs (PiBSs), and femto access points

⁹Alpha-stable distributions generalize Gaussian distributions and have heavier tails [10, Sec. 5.1], [12].

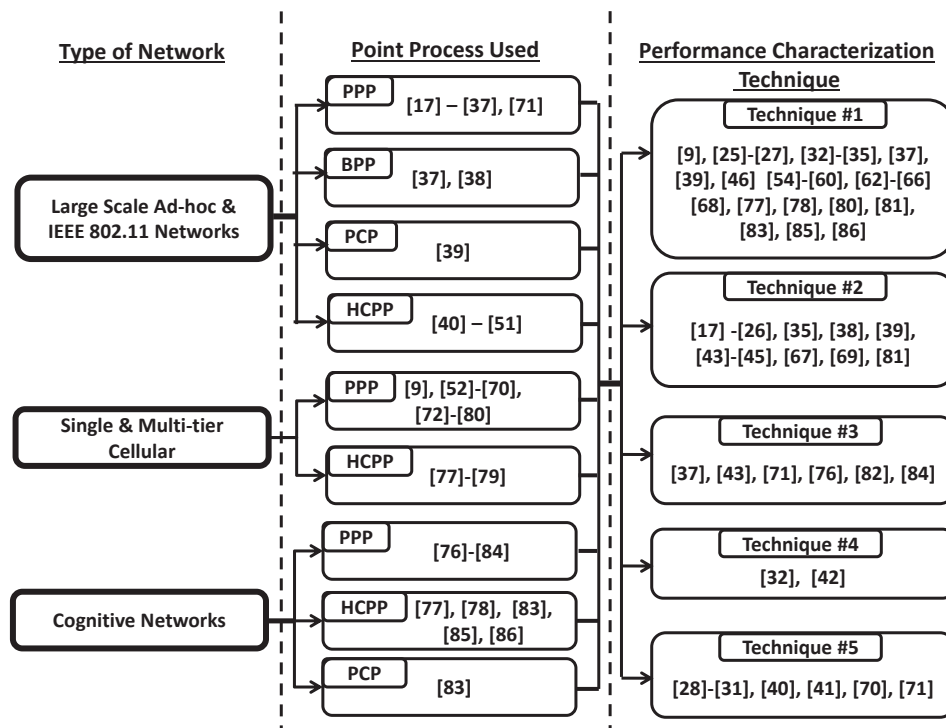


Fig. 4. Taxonomy of the related work on stochastic geometry-based modeling of wireless networks.

(FAPs))¹⁰. Small cells are deployed in the high traffic spots of the cellular networks to satisfy the high traffic demand. Some of the small cells such as the femto cells are installed and operated by the users. Femto cells are small access points mainly installed indoors to enhance indoor coverage. Femto cells may be installed by the operator to enhance poorly covered spots or by users to enhance their indoor coverage. With small cells, more randomness and more interference are introduced to the cellular network. In the following, we first show the baseline models used to derive the outage probability and mean transmission rate of multi-tier cellular networks, then we will show how these simplified models are adapted to capture, model, and analyze more sophisticated network models.

A. PPP and HCPP Models

In the context of cellular networks, the hexagonal grid model is widely accepted and has been extensively used in the literature to model, analyze, and design traditional single-tier cellular networks. In the hexagonal grid model, it is assumed that the locations of the BSs follow a deterministic grid, each BS covers a hexagonal cell, and all cells have the same coverage area. Due to the complexity and analytical intractability of modeling inter-cell interference in the grid model, researchers have always used simplifications which make the accuracy of their models disputable [9], [54]. Moreover, due to the variation in capacity (both network and link capacities) demand across the service area, the locations of the

BSs significantly deviate from the idealized grid-based model [54].

Looking at the cellular networks at different locations (i.e., downtown, residential areas, parks, rural areas, etc.), we notice that the positions of the BSs exhibit random patterns. Hence, stochastic geometry can be used to model the locations of the BSs. Ideally, the locations of the BSs should be modeled via a repulsive PP to reflect the basic planning procedure used in cellular network deployment. That is, although the distances among the BSs are random, in a real (i.e., deployed) cellular network, we cannot find two BSs owned by same service provider arbitrarily close to each other. Therefore, a repulsive PP such as the Matérn HCPP with a hard core parameter that reflects the minimum acceptable distance between two BSs can be used to model the cellular network topology [92]. Fig. 5 shows the modeling of a cellular network via the hexagonal grid, the PPP, and the HCPP.

As shown in Fig. 5, with the PPP modeling, there could be some BSs arbitrarily close to each other. On the other hand, the grid-based model is too idealized. Instead, the HCPP provides a more realistic modeling at the expense of analytical tractability. Dealing with repulsive PPs is relatively more complicated and the Matérn HCPP suffers from some flaws (i.e., the nonexistence of the probability generating functional and the flaw of underestimating the intensity of the points that can coexist for a given hard core parameter) that are still being addressed by the research community [49], [51], [87], [88]. Therefore, the PPP is much more appealing due to its simplicity and tractability [11], [13], [14]. However, it seems impractical to assume that the locations of the BSs are completely uncorrelated. In [54], the authors compared the performance of a PPP and a square grid model to the performance of an actually deployed cellular network. Surpris-

¹⁰In this article, our main focus is on heterogeneous networks composed of a cellular network overlaid by small cells. This is different from that in [71] which models the coexistence between narrow band networks and ultra wide band networks.

TABLE I
TAXONOMY OF THE LITERATURE BASED ON THE NETWORK TYPE, POINT PROCESS USED, AND THE TECHNIQUE USED TO OBTAIN THE PERFORMANCE METRICS

Network Type	Used PP	Performance Evaluation Techniques				
		Technique #1	Technique #2	Technique #3	Technique #4	Technique #5
Ad hoc & IEEE 802.11	PPP	[25]–[27], [32]–[35]	[17]–[26], [35]	[71]	[32]	[28]–[31], [71]
	BPP	[37]	[38]	[37]	-	-
	HCPP	[46]	[43]–[45]	[43]	[42]	[40], [41]
	PCP	[39]	[39]	-	-	-
Single-tier & Multi-tier Cellular	PPP	[9], [54]–[60], [62]–[66] [68], [77], [78]	[67], [69]	[76]	-	[70]
	BPP	-	-	-	-	-
	HCPP	[77], [78]	-	-	-	-
	PCP	-	-	-	-	-
Cognitive	PPP	[77], [78], [80], [81], [83]	[81]	[76], [82], [84]	-	-
	BPP	-	-	-	-	-
	HCPP	[77], [78], [83], [85], [86]	-	-	-	-
	PCP	[83]	-	-	-	-

ingly, the PPP was observed to provide lower bounds on the coverage probability and the mean transmission rate obtained by measurements that are as tight as the upper bound provided by the idealized grid-based model. Further validations of modeling cellular networks via PPP can be found in [92], [93].

Although the idea of modeling the cellular network using the PPP goes back to the late 90’s [52], [53], the work in [54] brought much attention to this modeling approach due to the useful formulas derived for the performance metrics (such as the outage probability and the mean transmission rate), and comparison with the grid-based model and the actual system that revealed the accuracy of the PPP model. The relatively tight bounds provided by the PPP opened a new research direction to model, analyze, and understand cellular networks. With the vast amount of results on the PPP available in the literature along with its simplicity and tractability, it can be used to characterize and understand the behavior of cellular networks in terms of the various design parameters as will be shown later in the article.

B. Baseline Stochastic Geometry Models

The baseline models are simplified models that are used to understand and establish the analytical paradigm to be used in more practical and complicated cases. In this section, we will review the baseline stochastic geometry models for multi-tier cellular networks. In the baseline model, for the special case of a single tier cellular network, the locations of the BSs are modeled via a PPP. Assuming that all BSs transmit with the same transmit power and each user associates with one of the BSs based on the received signal strength (RSS), the coverage regions of the BSs forms a Voronoi tessellation¹¹ [94]. That is, a line bisecting the distance between each two

neighboring BSs will separate their coverage regions. The planar graph constructed by perpendicular lines bisecting the distances between the points of a PP is called a Voronoi tessellation. Fig. 5 shows the Voronoi tessellations for different point processes¹².

In [54], both the BSs and the users were modeled via independent homogeneous PPPs, and it was assumed that all BSs use the same frequency (channel). The users were assumed to associate based on the long term average RSS (i.e., to the nearest BS). The authors used the Rayleigh fading assumption (i.e., technique #1) to find the exact downlink coverage probability (i.e., $\mathbb{P}\{\text{SINR} \geq \theta\}$ where θ is the threshold for correct signal reception) and the average transmission rate for a test user added at the origin. Note that, according to Slivnyak’s theorem, the statistics seen from a PPP is independent from the test location [10], [13], [14]. Hence, no generality is lost in studying the statistics seen by the user added at the origin.

In [54], the average transmission rate is derived in the same manner as the coverage probability as follows:

$$\begin{aligned}
 \mathbb{E}[\ln(1 + \text{SINR})] &\stackrel{(i)}{=} \int_0^\infty \mathbb{P}\{\ln(1 + \text{SINR}) > t\} dt \\
 &= \int_0^\infty \mathbb{P}\{\text{SINR} > (e^t - 1)\} dt \\
 &\stackrel{(ii)}{=} \int_0^\infty e^{-Wc(e^t - 1)} \mathcal{L}_{I_{\text{agg}}}(c(e^t - 1)) dt
 \end{aligned} \tag{7}$$

where (i) follows because $\ln(1 + \text{SINR})$ is a strictly positive random variable, and (ii) follows from (5). Given that the Laplace transform of the aggregate interference associated with a PPP is available and easily computable, the mean transmission rate can be easily obtained by evaluating (7).

¹¹The Voronoi tessellation captures the hexagonal grid as a special case.

¹²Fig. 5 is plotted with Matlab via the command *voronoi*.

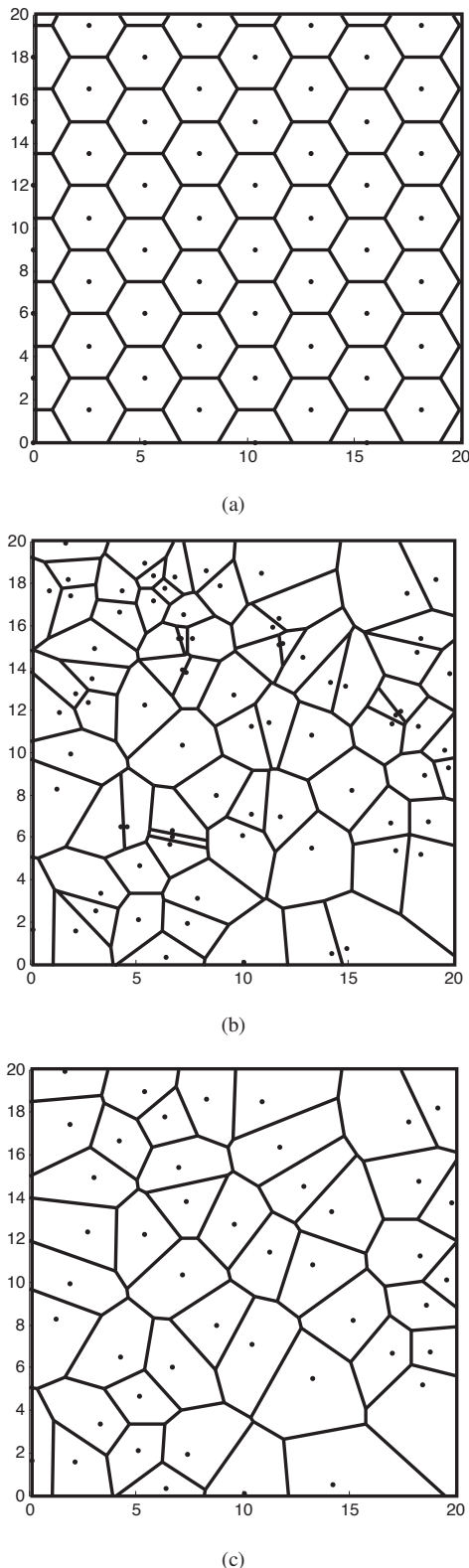


Fig. 5. (a) Cellular network modeled via the grid-based model, (b) Cellular network modeled via the PPP, (c) Cellular network modeled via the HC-PPP.

The main findings of [54] are: (a) the PPP provides a relatively tight bound for the performance of actual networks, (b) simple expressions can be derived for the coverage probability and mean transmission rate, (c) in interference-limited networks (i.e., the noise is negligible w.r.t. the interference and hence

is ignored), the signal-to-interference-ratio (SIR) statistics are independent of the intensity of BSs [54, eq. (25)].

It is quite insightful to see that in interference-limited networks (i.e., when noise is ignored), both the performance metrics (i.e., coverage probability and average rate) are independent of the intensity of the BSs. That is, increasing the intensity (number) of the BSs neither degrades nor improves the coverage probability within the cell and the average rate achieved by the users. This behavior can be explained as follows: as the intensity of the BSs increases, the average distance between the users and their serving BSs decreases which increases the desired signal power. On the other hand, the aggregate interference (i.e., inter-cell interference) increases with the same rate as the desired signal. Hence, the SIR remains constant. Therefore, the coverage probability and average rate can only be increased through interference management techniques such as frequency reuse, multiple-input-multiple-output (MIMO) antennas, or inter-cell cooperation. Although these results are only valid for the PPP network model, they are insightful because they reflect the worst-case network performance. More specifically, deploying more BSs, in the worst case, will never degrade the SIR statistics.

In [72], the lemma presented in [95] was used as an alternative way to evaluate the downlink mean transmission rate in cellular networks. In [95], an easy method that relies on the MGFs was proposed to evaluate averages in the form of $\ln \left(1 + \frac{\sum_{i=1}^N a_i}{\sum_{j=1}^M b_j + 1} \right)$, where a_i and b_j are random variables with arbitrary distributions. Note that a_i corresponds to the desired signal power (i.e., numerator of the SINR), while each of the b_j s corresponds to the power of an interference signal. [72] applied the MGF method developed in [95] to obtain the exact average transmission rate for the cellular network modeled via the PPP for Nakagami- m fading in the desired link (i.e., the Rayleigh fading assumption used in technique #1 is relaxed). However, this method is only valid for the transmission rate and is not applicable to evaluate the SINR distribution (i.e., the outage probability). The work in [54] for cellular networks was extended to a single cellular network consisting of K -tiers in [55], and to M -cellular networks each consisting of K -tiers in [56].

In multi-tier cellular networks, the coverage of each network entity depends on its type (i.e., an MBS, MiBS, PiBS or a FAP) and the network geometry (i.e., its location w.r.t. other network entities). That is, assuming that each user will associate with (i.e., is covered by) the network entity that provides the highest signal power, the coverage of each network entity will depend on its transmit power as well as the relative positions of the neighboring network entities and their transmission powers. For instance, if two MBSs have the same transmission power, a line bisecting the distance between them will separate their coverage areas. However, for an MBS with 100 times higher transmit power than a FAP, a line dividing the distance between them with a ratio of $(100)^{\frac{1}{\alpha}} : 1$ will separate their coverage areas, and so on. If the BSs in all the tiers are modeled via independent homogenous PPPs, due to the high variation of the transmission power of the BSs belonging to different tiers, the multi-tier cellular network coverage will constitute a weighted Voronoi tessellation. The

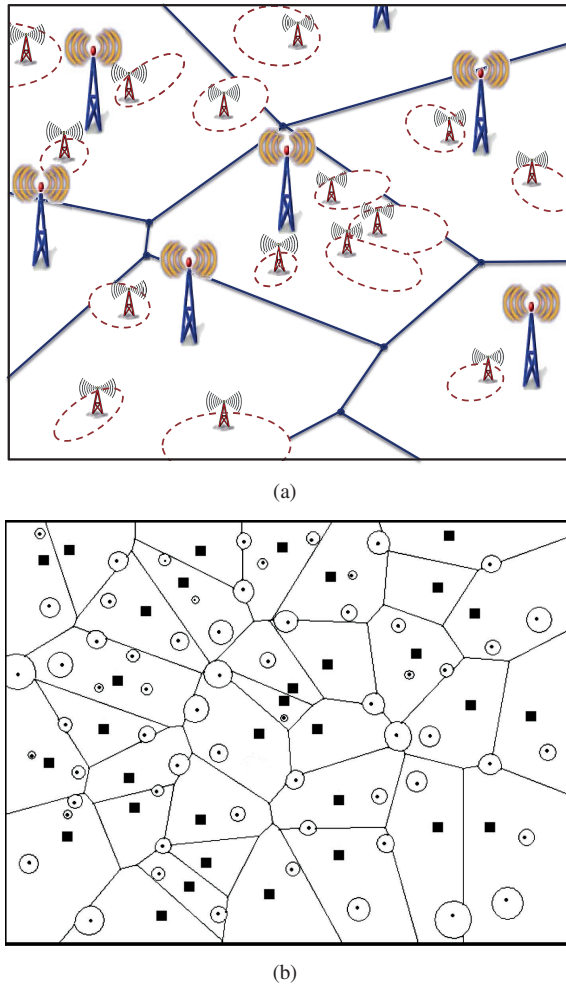


Fig. 6. (a) The HetNet model, (b) The network modeled as a weighted Voronoi tessellation (the square shapes represent the MBSs and the dots represent the SBSs).

weighted Voronoi tessellation is the planar graph constructed by bisecting the distances between the points of a PPP according to the ratio between their weights, where the weights are obtained based on the transmission powers of the BSs and the propagation condition (e.g., path-loss exponent).

Fig. 6 shows an example for the coverage of a two-tier cellular network and the corresponding weighted Voronoi tessellation. In [55], the authors modeled a multi-tier cellular network where all network tiers were assumed to follow independent homogenous PPPs and all tiers used the same frequency channel. The authors computed the tier association probability and the average tier load using the Rayleigh fading assumption (technique #1) to evaluate the coverage probability and the mean transmission rate assuming that the users connect to the BSs offering the highest long term average SINR. Note that, due to the assumption of independent PPPs, the aggregate interference received from each network tier is independent of the aggregate interferences received from other network tiers. It is worth mentioning that the SINR-based association is more complicated than the RSS-based association because it depends on both the desired RSS as well as the interference signal strength. The authors overcame this problem and proved that if the target SINR threshold is

greater than 1 (i.e., 0 dB), only one network entity can satisfy the SINR requirement [55, Lemma 1]. Hence, the probability that a user is covered is just the sum of the probabilities that the SINR from each network tier is satisfied. In [55], it was shown that the PPP assumption is accurate to within 1-2 dB of the measured coverage probability in an actual LTE network overlaid by heterogeneous tiers modeled as PPPs.

The assumption that only one BS can satisfy the target SINR (i.e., SINR threshold is greater than 0 dB) as well as the assumption that each BS allocates its total power to the test user, which were used in [55], were relaxed in [66]. In [66], the author assumed a more realistic case where the total transmit power of the BS is shared among the served users and that the user connects to the network entity providing the highest instantaneous SINR, although the instantaneous SINR can be satisfied by more than one tier. Under the modified network model, the author in [66] derived the joint complementary *cdf* (*ccdf*) of the SINR measured at an arbitrary user from the set of candidate network entities (i.e., the nearest BS from each network tier) in a general K -tier HetNet. The author also used the Rayleigh fading assumption (i.e., technique #1) to obtain an exact closed-form expression for the joint *ccdf* (i.e., association and coverage probability).

Different from the downlink analysis in [54], [55], [66], [72], the uplink analysis is significantly more involved due to the per user power control. In [57], the authors assumed that the BSs and the users follow independent PPPs and used the Rayleigh fading assumption (i.e., technique #1) to evaluate the uplink coverage probability when the users are employing fractional channel inversion power control.

Although the basic network models are very simplified (i.e., not very practical), they provide a simple yet accurate and robust baseline analytical paradigm for modeling and analysis of multi-tier cellular networks. As we will see later, many research papers are building on these simple models to provide more practical and more rigorous models for multi-tier cellular networks.

C. Stochastic Geometry Models for Frequency Reuse in Cellular Networks

Incorporating frequency reuse in a stochastic geometry model is challenging because it introduces correlation among the BSs using the same frequencies. Hence, the tractability of the PPP will be partially lost (i.e., neighboring BSs should be using different frequency sub-bands).

In [54], the authors overcame this problem and kept the properties of PPP by modeling the worst-case frequency reuse in cellular networks. That is, they assumed that each BS would randomly and uniformly pick one of the available frequency sub-bands to use. Since independent thinning of a PPP leads to another PPP [10], the network model after frequency reuse is also a PPP. Hence, applying frequency reuse is equivalent to applying independent thinning to the complete set of interfering BSs. If the network has BSs with intensity λ and each BS randomly and uniformly picks one of the Δ available sub-bands, the BSs using the same sub-band constitute a PPP with intensity $\frac{\lambda}{\Delta}$. Therefore, the intensity of the interfering BSs will be $\frac{1}{\Delta}\lambda$.

Although, as discussed in the previous section, it was concluded in [54] that the intensity of the BSs affects neither the coverage probability nor the average rate (since both the user association and interference change with the BS intensity), exploiting frequency reuse will affect both the performance metrics. This is because frequency reuse will decrease the interference without changing users' association to the corresponding serving BSs. That is, while a typical user will be served from one of the complete set of BSs with intensity λ , she will experience interference only from BSs using the same frequency sub-band with intensity $\frac{1}{\Delta}\lambda$. Hence, there is no contradiction between the results obtained for the frequency reuse and the result that both the coverage probability and the average rate are independent of the intensity of the BSs. Frequency reuse will increase the coverage probability at the expense of decreasing the average achievable rate because only $\frac{1}{\Delta}$ of the spectrum is available per BS.

Applying traditional frequency reuse decreases the aggregate interference and enhances the coverage probability at the expense of reduced area spectral efficiency due to the reduced frequency usage per unit area. Fractional frequency reuse (FFR) is a potential solution to enhance the SINR statistics of the poorly covered users (i.e., edge users) while maintaining high frequency reuse [96]. In FFR, the cells are spatially partitioned (i.e., into inner cell region and edge cell region, and/or sectors by directional antennas), and different frequency sub-bands are assigned to different spatial regions of a cell to enhance the cell edge coverage while maintaining the high frequency reuse.

There are two main types of FFR, namely, strict FFR and soft FFR. In strict FFR, the frequency band is divided into $\Delta + 1$ sub-bands. One large sub-band is assigned for all cells to be used in their inner cell region and Δ relatively smaller sub-bands are alternated between the cell edges of neighboring cells such that no two adjacent cell edges use the same frequency sub-band. Hence, an edge user will experience interference from only the subset of BSs using the same edge sub-band which are relatively far BSs. On the other hand, the soft FFR divides the spectrum into Δ sub-bands and all sub-bands are used in all cells with power control. That is, in each cell, $\Delta - 1$ sub-bands are used in the inner cell region and one sub-band is used in the cell edge region such that neighboring cells do not use the same edge sub-band. The BSs transmit in the inner sub-bands with power P_1 and in the edge sub-band with power P_2 such that $P_2 > P_1$. Hence, an edge user will have a higher desired signal power and a relatively lower interference power.

In the context of stochastic geometry, it is very tricky to include the FFR schemes into the network model for two reasons. The first reason is that the Voronoi cells have random shapes, which makes it difficult to find a criterion to define the spatial cell partitioning (i.e., inner and edge regions) and expressions for the areas of cell partitions¹³. The second reason is that FFR brings spatial correlations among the BSs using the same sub-band in the cell edge which violates the PPP assumption.

In [62], [63], the authors overcame the above problems and

extended the model in [54] and [55] to include FFR in single and multi-tier cellular networks. The authors overcame the first problem by partitioning the users as the cell edge users and the inner cell users by an SINR threshold rather than by their spatial locations. That is, if the SINR of a user is above a certain threshold T_{thr} , she is considered as an inner user. Otherwise, she is considered to be an edge user. For the second problem, as in [54], the authors avoided the spatial correlations introduced by the FFR by considering the worst-case FFR. That is, each BS randomly and uniformly chooses one of the sub-bands for the edge users. Hence, the BSs using the same sub-band as an edge sub-band is a PPP with intensity $\frac{1}{\Delta}\lambda$. With these assumptions, the FFR can be captured in the system model by simple modifications in the expression for SINR as discussed below.

In the strict FFR case, the inner users will have the same interference statistics as in the no FFR case. On the other hand, the edge users will have interference from a thinned PPP with intensity $\frac{1}{\Delta}\lambda$. For the soft FFR, both edge and inner users will experience the same interference. However, the edge users will have a signal with higher power (due to higher P_2). Both [62], [63] used the Rayleigh fading assumption (i.e., technique #1) to quantify the FFR performance gain over the no reuse and traditional frequency reuse in terms of the outage probability and mean transmission rate. The authors also analyzed the tradeoffs between the two FFR schemes. Note that both [62], [63] only accounted for a simplistic FFR with only two regions (i.e., inner and edge), and the cell sectorization was not taken into account.

D. Spectrum Allocation in Two-tier Cellular Networks

In the context of multi-tier cellular networks, spectrum sharing (i.e., universal frequency reuse) increases the area spectral efficiency at the expense of higher cross-tier interference. On the other hand, spectrum partitioning eliminates cross-tier interference at the expense of lower area spectral efficiency. The analysis of the tradeoff between spectrum sharing and partitioning is of primary interest to the researchers to obtain optimal operation of multi-tier cellular networks.

Optimal spectrum sharing in a two-tier cellular network in the downlink was investigated in [67], [68], while spectrum sharing in the uplink was investigated in [70]. In [67], the available spectrum is partitioned into two groups, one group of channels is assigned to the macro tier and the other group of channels is assigned to the femto tier to eliminate cross-tier interference. In [67], the authors derived the optimal spectrum partitioning that maximizes the area spectral efficiency subject to a network-wide minimum rate requirement. The MBSs were modeled via a hexagonal grid-based model, while the FAPs were modeled using a homogenous PPP model. The authors used the region bounds (i.e., technique #2) to find a tight lower bound on the SINR and hence the transmission rate. The authors also proposed a randomized spectrum access control called frequency ALOHA (F-ALOHA) for the FAPs. In F-ALOHA, each FAP accesses each of the available frequencies independently with probability p . The F-ALOHA spectrum access presents a tradeoff between the spatial frequency reuse and the aggregate interference in the femto-tier network. The

¹³FFR allocations for Voronoi tessellations were discussed in [97].

authors in [67] showed that, due to the increased interference, the optimal p is a non-increasing function of the FAP intensity.

Since spectrum partitioning reduces the area spectral efficiency, it may not be the optimal spectrum allocation scheme even if the share of the coexisting networks is optimized. In [68], the authors studied the spectrum sharing/partitioning tradeoffs and aimed at deriving the optimal spectrum allocation scheme that maximizes the transmission capacity subject to an outage probability constraint in a two-tier cellular network (i.e., MBSs overlaid by FAPs). Unlike [67], the authors investigated both joint and disjoint spectrum sharing for two-tier cellular networks. That is, assuming that there are C available channels to be shared among both network tiers, the authors investigated whether it is optimal to have both network tiers jointly share the entire channels or to disjointly divide the available channels among the two tiers. The authors used PPP modeling for both the network tiers and the Rayleigh fading assumption (i.e., technique #1) to derive the outage probability and mean transmission rate to optimize the spectrum allocation scheme. It was shown that joint allocation is optimal for sparse network deployments while disjoint allocation is optimal in dense network deployments.

For the uplink case, the authors of [70] derived the network capacity region of a two-tier cellular network consisting of MBSs modeled via the hexagonal grid, FAPs modeled via PPP, and users modeled via an independent PPP. The network capacity region is defined as all combinations of the intensities of users of the two networks that satisfy an outage constraint. The system model considered in [70] accounts for sectored antennas, spread spectrum transmission, and power control via channel inversion. Due to the small transmission radius of the FAPs, the interference seen from all users served by the same FAP was approximated by an isotropic point source of interference with the worst-case sum transmission powers of the FAP users. The aggregate interference seen from all FAP users is approximated by the aggregate interference seen from a PPP modeling the location of the FAPs, hence the aggregate interference from the femto tier can be calculated via the inversion method (technique #5). The authors showed that spectrum sharing with sectored antennas along with time hopping spread spectrum boosts the network capacity of the system by a factor of seven relative to the spectrum partitioning with omni-directional antennas. However, since the analysis in the paper is based on the worst-case scenario, only very pessimistic bounds on the performance metrics can be obtained.

Spectrum sharing between a cellular network uplink and a mobile ad hoc network was investigated in [69]. The authors compared the tradeoff between overlay and underlay spectrum sharing for the uplink channels of the cellular network. It was assumed that the transmitters in both networks use frequency-hopping spread spectrum to transmit their signals and that the cellular network controls the spectrum sharing method. The BSs of the cellular network, the ad hoc transmitters, and the cellular network users follow independent PPPs. The authors used the bounding technique (technique #2) to find upper and lower bounds on the outage probability as well as the transmission capacity with and without successive interference cancellation. The authors also determined the capacity regions

for the networks. In contrast to the two-tier cellular network analyzed in [70], in the case of spectrum sharing between a cellular network uplink and a mobile ad hoc network, it was shown that spectrum partitioning outperforms the spectrum sharing allocation. One explanation for this result is that different tiers in a multi-tier cellular network complement each other. That is, each user associates with the best network entity (i.e., the best in terms of SINR or RSS) from the different coexisting tiers, hence, individual interference sources are usually weaker than the intended transmission source (see Fig. 1). On the other hand, in the cellular network overlaid by a mobile ad hoc network, the two networks are completely disjoint and there are no bounds on the locations of the interference sources. Hence, spectrum partitioning is optimal in the latter case.

E. Biasing and Load Balancing in Multi-tier Cellular Networks

In multi-tier cellular networks, choosing the appropriate network tier to associate with is a non-trivial problem [98], and a simple RSS- or an SINR-based network selection scheme may not be optimal. As shown earlier (see Fig. 6), the coverage of each network element highly depends on its type and the network geometry. Therefore, there are significant differences in the size of the coverage areas of the different network elements, which may result in high diversity in the loads served by the different network elements. The high diversity of cell loads in a K -tier cellular network was analyzed in [58]. The authors showed that due to the high diversity of the loads served by the coexisting network elements, some network elements might be idle and hence would not contribute to the aggregate interference. Therefore, the authors in [58] upgraded the SINR model in [55] (i.e., used PPPs with technique #1) to account for the activity factor of the coexisting heterogeneous BSs. It was shown that adding lightly-loaded femto and pico cells to the network increases the overall coverage probability. However, due to the random deployment of the small cells along with the high transmission power gap with the MBSs, there might be some overloaded network elements (i.e., network elements with high transmit powers) and a large number of un-utilized small cells. That is, since a user associates with one of the coexisting network tiers based on the RSS, the load per network tier is hard to control since it depends on several factors such as the relative transmission power and the intensity of the BSs belonging to each network tier. Hence, according to the network configuration, we may end up with some congested tiers and under-utilized tiers.

In [59], [60], the authors investigated the above issue and introduced a parameter called the biasing factor to control the network load of each network tier. The biasing factor is used to bias the users to associate with a given network tier even if it does not provide the strongest signal power (or equivalently the strongest SINR). The biasing can be viewed as a virtual increase in the relative transmit power of the given network tier. Biasing is also widely known as range expansion in the 3GPP standards and proposals [99], [100]. Note that biasing will affect the interference geometry by changing the minimum separation distance between a user and

its interfering sources. That is, as shown in Fig. 1, given that the distance between a small cell user and its serving SBS is r , the minimum separation between that user and an interfering MBS will be $r_m > r \left(\frac{P_m}{P_s T} \right)^{\frac{1}{\eta}}$, where $T \geq 1$ is the bias factor.

In [59], [60], the authors used the Rayleigh fading assumption (i.e., technique #1) to calculate the outage probability, the average transmission rate, and the minimum achievable rate for the users. It was shown that while no biasing is optimal for outage and average transmission rate, biasing increases the minimum achievable rate for the users. These results can be explained as follows.

With biasing, according to the given network configuration, we can redistribute the users across the network tiers as uniformly as possible, hence, the load per highly loaded network entity decreases, and the *minimum* rate of each user increases. Since in [59], [60] only one channel is assumed and biasing forces users to associate with network entities that do not provide the highest SINR, it is intuitive (specially with the single channel assumption) that the outage probability will increase and the *mean* transmission rate will decrease due to the degraded SINR performance per user.

For a two-tier HetNet, in [61], the authors examined different techniques that can be used to offload users from one network tier to another and their effect on the activity factor (i.e., the probability of being idle) of the coexisting network elements in order to efficiently control the load in each tier. It was shown that the user association probability to a specific network tier is more sensitive to the intensity of the BSs in that tier than the transmission power or biasing towards that tier. For instance, it was shown that a 10 dB power gap between the MBSs and the FAPs can be compensated for by a 5 dB increase in the intensity of the FAPs over the intensity of MBSs to have equal user loads associated to each network tier.

F. Optimal Deployment, Network Expansion, and Power Saving in Multi-tier Cellular Networks

Stochastic geometry modeling can be exploited to find the optimal network expansion policy (i.e., the optimal intensity and types of BSs to be deployed) in case of increased traffic demand, and the optimal intensity and types of BSs that could be switched off for power saving in case of reduced traffic periods.

In [64], the authors derived the minimum BS density subject to a minimum QoS constraint in a single-tier cellular network as well as in a two-tier cellular network composed of MBSs overlaid by MiBSs. The MBSs, MiBs, and the users were modeled via independent PPPs, and the Rayleigh fading assumption (technique #1) was used to derive the outage probability and the mean transmission rate. The authors in [64] used the relation between the number of users, the cell sizes, and the transmission rate to optimize the intensities of MBSs and MiBSs. That is, assuming universal frequency reuse and that the available spectrum is equally divided among the users served by each network entity, the transmission rate of each user is a function of the total number of users served by his serving network entity, which in turn is a function of

its transmission power, the intensities of the other network entities and their locations (as shown in Fig. 6).

For a single-tier cellular network, the optimal intensity of BSs can be found by solving the following optimization problem:

$$\begin{aligned} & \text{minimize} && \lambda \\ & \text{subject to} && \mathbb{P} \left\{ \frac{B}{\mathcal{N}} \ln(1 + \text{SINR}) < u \right\} < v \end{aligned} \quad (8)$$

where B is the total available bandwidth, $\mathcal{N} \sim \text{Poisson}(\lambda_u V)$ is the total number of users served by a given BS, λ_u is the intensity of the users, and V is the area of the coverage region (Voronoi cell) of the tagged BS. For interference-limited networks, using (5), the constraint in (8) can be rewritten as $\left[1 - \mathcal{L}_{I_{\text{agg}}} \left(e^{\frac{\mathcal{N}u}{B}} - 1 \right) \right] < v$ which can be obtained by the standard stochastic geometry analysis. It can be observed that the mean achievable rate of each user is an increasing function of λ , because as λ increases, the mean area of a Voronoi cell ($= \frac{1}{\lambda}$) [94] decreases (the plane is divided into more BSs) and the number of users served by each BS decreases. Note that increasing the intensity of the BSs does not affect the SIR statistics as shown earlier [54]¹⁴. Hence, (8) optimizes the tradeoff between the share that each user takes from the spectrum, and the intensity of deployed BSs. The authors extended this concept to a two-tier HetNet and obtained the optimal network expansion policy if the QoS of the users is not satisfied.

G. Stochastic Geometry Models for Access Policy in Small Cells

There are two main spectrum access policies for small cells (e.g., femto cells) in a multi-tier cellular network, namely, the open-access and closed-access policies. On one extreme, the open-access small cells accept to serve any cellular user. On the other extreme, the closed-access small cells only accept its own users called the closed subscriber group. Open-access small cells enhance the overall network coverage and mean transmission rate but do not guarantee the QoS for a specific group of users (e.g. femtocell owners). On the other hand, closed-access small cells can guarantee the QoS for the closed subscriber group at the expense of degrading the performance of non-subscribers. Note that closed access small cells may also experience significant interference from the non-subscribers [101].

In stochastic geometry modeling, from the perspective of an unsubscribed user, a closed-access policy may be looked at as the dual of the frequency reuse. That is, in frequency reuse [54], the user can associate with the complete set of BSs while experiencing interference from only a subset of the PPP (i.e., a PPP thinned with the frequency reuse). On the other hand, in a multi-tier cellular network with open and closed-access small cells, the non-subscribers to closed-access femto cells can associate with only a subset of the BSs (i.e., MBSs and open-access small cells) while experiencing interference from the complete set of BSs. Therefore, closed-access small cells generally degrade the performance of multi-tier cellular

¹⁴Note that the mean transmission rate of the BSs is still independent of the intensity of the BSs as shown in [54].

networks [55]. Hybrid channel access is considered as a potential solution to control the tradeoff between the overall network performance and the QoS guarantee for the closed subscriber group.

In hybrid-access small cells, the available spectrum is partitioned into two groups. One group is assigned to the closed subscriber group to guarantee their QoS, while the other group is assigned to the non-subscribers to enhance their coverage and reduce the interference experienced from them. In [65], the authors optimized the hybrid-access policy in a two-tier HetNet. That is, the authors found the optimal number of accessible channels for non-subscribers subject to a tolerable degradation for the small cells' closed groups of subscribers. The authors used independent PPPs to model the MBSs, the FAPs, the macro users, the non-subscribed users, and the closed group subscribers, and used the Rayleigh fading assumption (i.e., technique #1) to find the coverage probability and mean transmission rate. It was shown that if the optimal number of channels are left open for unsubscribed users, significant improvements for non-subscribed users can be achieved with a negligible performance degradation for the closed group of subscribed users. However, the model in [65] does not capture the offloading effect (i.e., the amount of decreased interference) by accepting non-subscribers to be served by the FAPs which might improve the performance of the closed subscribers.

H. Stochastic Geometry Models for Multiple Input Multiple Output (MIMO) Systems

Multiple-input-multiple-output (MIMO) systems will be key enablers for high-speed communications in LTE and LTE-Advanced networks. Incorporating MIMO into the model will increase the complexity of analysis. For instance, the simplistic Rayleigh distribution assumption for the channel power gains in a single-antenna system is not practical in the MIMO case because the interference power as well as the desired signal power distributions will depend on the MIMO configuration used. Moreover, different network tiers may use different MIMO configurations which will increase the complexity of the tier association problem. That is, the association probability is not just a function of the ratio of transmission power for the different network tiers. Instead, the association will depend on both the MIMO configuration as well as the transmit power. Furthermore, the condition that only one network entity can satisfy the SINR threshold for a given user (for SINR thresholds greater than 0 dB [55], [66]) will not hold.

In [73], the authors used stochastic geometry techniques developed in [24] to characterize the interference, and hence, the downlink coverage and rate in a given cell for a MIMO-based single-tier as well as multi-tier cellular network. That is, instead of deriving the system-wide spatial averages for the performance measures as in [54], [55], the authors derived the spatial averages for the coverage probability as well as the link capacity over a given cell with a known radius and interference protection region. The main idea in [73] for interference characterization is based on the result in [24], where it was shown that, for some MIMO configurations, the

distribution of the channel (power) gain in the desired link can be represented in the following form:

$$\mathbb{P}\{h_0 > x\} = \sum_n \sum_k a_{n,k} e^{-nx} x^k \quad (9)$$

and hence, the SIR distribution can be obtained from the Laplace transform as in the equation at the top of the following page, where (i) follows from (9) and (ii) follows from the identity $t^n f(t) \xrightarrow{LT} (-1)^k \frac{d^k \mathcal{L}_f(t)(s)}{ds^k}$. Hence, the SIR statistics can be obtained directly from the Laplace transform as in the case of Rayleigh fading single antenna channel (i.e., technique #1).

An important distribution satisfying (9) is the Erlang distribution. It was argued in [74] that, if a MIMO channel is impaired by Rayleigh fading, both the power from the desired link and powers from the interference links follow the Erlang distribution. More specifically, the channel power gain in the desired link will follow the gamma distribution $Gamma(\rho_k, 1)$ and that in the interference links will follow the gamma distribution $Gamma(\delta_j, 1)$, where ρ_k and δ_j are positive integers that depend on the applied MIMO technique applied and the number of antennas. If the channel power gain has a gamma distribution $h_0 \sim Gamma(\alpha, \beta)$ ¹⁵, where α and β are the shape and rate parameters, respectively, then for integer values of α , the distribution of h_0 matches the Erlang distribution and can be represented in the form of (9) as follows:

$$\mathbb{P}\{h_0 > x\} = \frac{\Gamma(\alpha, \alpha\beta)}{\Gamma(\alpha)} = e^{-\alpha\beta} \sum_{k=1}^{\alpha-1} \frac{(\alpha\beta)^k}{k!} \quad (10)$$

where $\Gamma(\cdot, \cdot)$ is the upper incomplete gamma function. The authors in [74] used the union bound along with the technique used in [24], [73] to obtain an upper bound on network-wide (i.e, not for a given cell as in [73]) coverage probability in a K -tier cellular network¹⁶.

Since the interference characterization technique used in [24], [73], [74] is limited to channel power gains that can be represented in the form of (9), in [75], the authors proposed the gamma distribution (i.e., technique #3) to approximate the interference in a MIMO multi-tier cellular network with system model similar to the one assumed in [73]. The authors in [75] used the moments obtained via the Laplace transform of the aggregate interference to approximate its *pdf* using the gamma distribution. The accuracy of the gamma approximation in [75] was validated by simulations.

V. STOCHASTIC GEOMETRY MODELS FOR COGNITIVE NETWORKS

It is a well established fact that rigid spectrum allocation significantly degrades the spectrum utilization¹⁷. Therefore, cognitive radio techniques, where a licensed spectrum band is opportunistically utilized by cognitive users (called secondary users), has been a hot topic of research. In the context of

¹⁵A gamma distributed channel power gain corresponds to the Nakagami- m fading.

¹⁶The upper bound is due to the union bound.

¹⁷Rigid spectrum allocation divides the entire available spectrum into sub-bands which are permanently allocated to some network entities for their exclusive usage.

$$\begin{aligned}
\mathbb{P} \left\{ \frac{P_t A h_0 r^{-\eta}}{I_{\text{agg}}} > \theta \right\} &= \mathbb{P} \left\{ h_0 > \frac{r^\eta I_{\text{agg}} \theta}{P_t A} \right\} \\
&\stackrel{(i)}{=} \mathbb{E} \left[\sum_n \sum_k a_{n,k} \left(\frac{\theta r^\eta}{P_t A} \right)^k I_{\text{agg}}^k e^{-\frac{n \theta r^\eta I_{\text{agg}}}{P_t A}} \right] \\
&\stackrel{(ii)}{=} \sum_n \sum_k a_{n,k} \left(-\frac{\theta r^\eta}{P_t A} \right)^k \frac{d^k \mathcal{L}_{I_{\text{agg}}}(s)}{ds^k} \Big|_{s=\frac{n \theta r^\eta}{P_t A}}
\end{aligned}$$

multi-tier cellular networks, the objective of cognitive radio is different from the conventional cognitive radio networks (i.e., cognitive networks with licensed and unlicensed users). That is, in conventional cognitive networks, the licensed band is opportunistically utilized by unlicensed networks subject to a tolerable performance degradation for the primary network. In contrast, in multi-tier cellular networks, there is no notion of priority because both cognitive network tiers and non-cognitive network tiers are licensed to use the spectrum. In multi tier cellular networks, cognitive radio-based distributed spectrum access techniques can be developed to improve the spectrum utilization, reduce interference, and enable the small cells to have self organizing network (SON) capabilities. Cognitive spectrum access in cellular networks will reduce the CAPEX and the OPEX for the network operators [3]–[5]. Therefore, all the design tradeoffs between the cognitive and non-cognitive network tiers can be optimized so that the overall performance of the cellular network can be optimized [77], [80].

Although the objective of cognition in conventional cognitive networks differs from that in cognitive cellular networks, stochastic geometry models that characterize interference in the conventional cognitive networks can be adapted for the cellular networks. Therefore, in this section, we will first review some stochastic models for conventional cognitive networks since they contain the basic foundations to be extended for multi-tier cellular networks. Then, we will review the few works that exist in the literature for multi-tier cognitive cellular networks.

A. Stochastic Geometry Models for Conventional Cognitive Networks

A simple primary network comprised of one primary link and a secondary network modeled as a PPP was considered in [81], [82], [84]. In [82], the aggregate interference from the secondary network on the primary receiver with an exclusion region was characterized. The authors assumed a PPP distribution for the secondary users and characterized the interference by approximating its *pdf* and *ccdf* using the Edgeworth expansion, the log-normal distribution, and the shifted log-normal distribution (i.e., technique #3). It was shown that the shifted log-normal approximation outperforms the other approximation (i.e., Edgeworth expansion and the log-normal distribution) schemes.

In [84], the aggregate interference from the secondary users (modeled as PPP) to a primary receiver was modeled. It was assumed that the primary link operates in the full-duplex

mode, hence, by listening to the uplink, the location of the primary receiver can be estimated. [84] obtained the characteristic function of the interference and generated the cumulants to approximate the *pdf* of the aggregate interference caused by the secondary network (technique #3) by a truncated alpha-stable distribution. The model in [84] accounts for shadowing, small-scale fading, and power control. However, in a half-duplex network, the primary receiver is idle, and its location cannot be estimated.

Unlike [84], in [81], the secondary users control their spectrum access w.r.t. the primary transmitter rather than the primary receiver. Therefore, the set of active secondary users constitutes a PPP outside the exclusion region (which is random due to fading) of the primary transmitter. [81] aimed at deriving the maximum intensity of secondary users that satisfy the outage constraint for the primary link. The authors used the Rayleigh fading assumption (technique #1) to find the exact results for the outage probability of the primary link as well as the mean transmission rate of the secondary users. To relax the Rayleigh fading assumption and account for shadowing effects, [81] also proposed an approximation based on the lower bound obtained by considering only the strongest secondary interferer (i.e., technique #2). [81] also analyzed the effect of power control, imperfect sensing, and cooperative sensing on the secondary and primary links. However, only one primary user was assumed.

The effect of multiple primary users was analyzed in [83]. In [83], a cognitive network composed of multiple primary users scattered as a PPP and multiple secondary users scattered according to an independent PPP in the spatial domain was modeled. The main focus in [83] was to characterize the aggregate interference in the cognitive network where secondary users are only allowed to transmit outside the exclusion region of the primary users. It was shown that the active secondary users form a Poisson hole process, which is a special case of the doubly stochastic Poisson process or the Cox process [10, Sec. 3.3]. That is, the active secondary users form a PPP existing outside the exclusion regions of the primary users. Since the Poisson hole process is hard to characterize, [83] obtained bounds on the aggregate interference by approximating the Poisson hole process with a PPP existing outside the exclusion region of the test primary user. [83] also proposed an approximation based on the PCP for the active cognitive devices and showed that it is quite accurate. The main performance metric in [83] is the outage probability, and the Rayleigh fading assumption (technique #1) was used to evaluate it. However, in [83], a secondary user does not consider transmissions from other secondary users, which may

lead to a significant performance degradation for the secondary users.

The two references [85], [86] accounted for the secondary transmission in a network with multiple-primary and multiple-secondary users. [85], [86] proposed a cognitive carrier-sense multiple access (C-CSMA) protocol for a cognitive radio network composed of primary users and secondary users modeled via a PPP. The C-CSMA protocol coordinates both the primary and secondary spectrum access by sequential contention resolution processes. That is, each time interval is divided into three time slots. The primary users contend for spectrum access in the first time slot and transmit in the second and third time slots, while the secondary users listen to the spectrum in the first time slot to monitor primary users, contend for spectrum access in the second slot if no primary user is active, and transmit in the third time slot. With the C-CSMA protocol, the locations of primary and secondary users accessing the spectrum are correlated and hence are modeled via the HCPP. [85], [86] aimed at calculating the spectrum access probabilities, the outage probabilities as well as the transmission capacities. The Rayleigh fading assumption (technique #1) was used to derive approximate expressions for the outage probabilities as well as the transmission capacities¹⁸. The effect of request-to-send and clear-to-send (RTS-CTS) handshaking was analyzed in [85] while the multicast and broadcast variations of the network model were analyzed in [86].

B. Stochastic Geometry Models for Multi-tier Cognitive Cellular Networks

In the context of multi-tier cellular network, as shown in [68] and discussed in Section IV-D of this article, the optimal spectrum allocation (i.e., joint or disjoint and the optimal partitioning) depends on the intensity of BSs which may vary across the service area. Furthermore, it is infeasible (in terms of complexity and delay) to have a centralized controller for resource allocation to maximize the frequency utilization and mitigate interference between the coexisting network elements. Therefore, cognition via spectrum sensing is foreseen as a potential distributed solution for spectrum access. That is, cognition provides a potential solution for dynamic spectrum allocation which will adapt to the network geometry and maximize the spatial frequency reuse.

A two-tier cellular network with cognitive FAPs was analyzed in [76]. The network model considered is composed of a single MBS, a single primary user, and multiple cognitive FAPs. It was assumed that the macro user generate a busy tone to reserve the channel so that the cognitive FAPs can estimate the link quality towards the macro receiver. A FAP defer its transmission if it receives the the busy tone generated by the macro user with a power greater than a certain threshold. Hence, an interference protection region can be guaranteed around the macro user. The authors in [76] used the cumulants (obtained via the characteristic function of the aggregate interference) to approximate the *pdf* (technique #3) of the aggregate interference using log-normal and shifted

log-normal distributions. The authors obtained the outage probability and the average transmission capacity and used simulations to show the accuracy of their model.

In [77], a two-tier cellular network composed of multiple MBSs, multiple cognitive FAPs, multiple users in a multiple channels environment was modeled. The MBSs, FAPs, and users were modeled via independent PPPs. The cognitive FAPs use a CSMA protocol which is similar to the C-CSMA protocol proposed in [85], [86] to avoid interference with primary users as well as secondary users. Therefore, the active cognitive FAPs form an HCPP. The Rayleigh fading assumption (technique #1) was used to derive the outage probability and quantify the gain in outage probability due to the cognition of the FAPs. It was shown that cognition in a two-tier cellular network can decrease the outage probability by as much as 60% (for example, from 75% to 15%).

In [78], [79], it was shown that although cognition boosts the outage performance in a multi-tier cellular network, cognition w.r.t. all network tiers may not be optimal. That is, in a dense deployment scenario of small cells (e.g., FAPs), the spectrum opportunities will be very rare. Therefore, the performance gain in the SINR outage probability (due to the improvement in SINR) is wasted by the outage probability due to the opportunistic channel access. Hence, [78] proposed a semi-cognitive scheme for the FAPs, where the semi-cognitive FAPs only avoid interfering with the MBSs due to the high transmit power gap and they aggressively use the channels used in the femto network tier. It was shown that although the aggregate interference in the semi-cognitive scheme is higher than the aggregate interference in the full-cognitive scheme, the overall outage performance of the semi-cognitive scheme is better due to the increased spectrum opportunities.

In [80], the authors investigated the effect of different channel allocation schemes in the macro network tier on the opportunistic spectrum access probability for the cognitive small cell tier in a two-tier cellular network. It was shown that if each MBS independently of other MBSs allocates its channels based on the channel quality index of the users, the cognitive small cells will suffer from a deteriorated spectrum access performance. In contrast, if the MBSs follow a conservative channel allocation scheme to minimize the number of unique channels used by the macro network tier, the spectrum access performance of the cognitive SBSs will significantly improve, albeit at the expense of increased inter-tier interference in the macro tier. The authors in [80] also quantified the performance gain in terms of outage probability (via technique #1) achieved by the macro users when cognition is implemented in the SBSs. It was concluded that a conservative channel allocation scheme in the macro-tier along with cognition in the small cell tier achieve the required tradeoff between performances in the macro-tier and the small cell tier.

VI. FUTURE RESEARCH DIRECTIONS

In this section, we discuss possible extensions for stochastic geometry modeling in cellular networks. There are three main research directions for stochastic geometry modeling of multi-tier cellular networks. The first is to capture more practical system parameters in the system model. From the discussions

¹⁸Note that the approximation here is due to the non-existence of the Laplace transform of the HCPP as mentioned in Section II.

provided in Section IV, we see that the system models used in the literature are simplistic and do not account for actual system characteristics. For instance, most of the system models consider PPP distributed BSs, one channel, single antenna, and downlink transmission. Therefore, advanced system models that account for MIMO, multiple channels, different channel allocation strategies, power control, coordinated multi-point transmission, mobility, cognition, and uplink transmission are required. The second direction is to go beyond the coverage probability and the performance metrics based only on the Shannon's formula. For instance, if the queuing dynamics can be incorporated in the analysis, useful performance metrics such as the transmission delay can be obtained. The third direction is to adopt point processes that capture the characteristics of cellular networks with more accuracy and thus provide better modeling approaches. A detailed discussion on these potential research directions is provided below.

Although spatial randomness in the topology is an intrinsic characteristic of both large-scale ad hoc networks and cellular networks, sophisticated distributed MAC protocols in ad hoc networks as well as sophisticated planning and interference management protocols in cellular networks bring some structure to the network topology. That is, the independence assumption for the positions of simultaneously active transmitters is not realistic. Hence, the repulsive point processes such as the Matérn HCPP provide more realistic and accurate modeling for wireless networks.

In [92] the authors examined four point processes to find which of them better models the spatial distribution of an actual cellular network, namely, the PPP, the HCPP, the Strauss process (SP), and the perturbed triangular lattice. The Strauss process belongs to the general class of Gibbs processes, which first appeared in statistical physics [10, Sec. 3.6]. It captures the pairwise interactions between nearby BSs by making it less likely that two BSs are located close to each other, i.e., Strauss processes are *soft-core* processes. The authors in [92] showed that, compared to the PPP, the three non-Poisson models can model the spatial locations of the deployed BSs more accurately. The Gibbs processes were also used in [102]. The authors compared the spatial characteristics of two actual cellular deployments in a coastal city and sprawling landlocked city to the spatial characteristics of the PPP, the hexagonal grid as well as to the Gibbs models, and it was shown that the Gibbs model, in particular the so-called *Geyer saturation process*, better captures (i.e., better than both the PPP and the hexagonal grid models) the spatial characteristics of the actual cellular deployments. However, the main problem with Gibbs processes is that they are not analytically tractable [10, Sec. 3.6].

The tractability issue of the Gibbs processes makes the HCPP of special interest. The HCPP is relatively more tractable than the Gibbs process and has been frequently used for modeling ad hoc networks and the existing results may facilitate its application in the context of cellular networks. However, there are some challenges that should be addressed for efficient and accurate modeling via the HCPP. The first challenge is to obtain a simple closed-form expression that accurately captures the intensity of the nodes that can coexist for a given hard core parameter. The known closed-

form expression (for the MHCPP type II), which has been extensively used in the literature, underestimates the intensity (i.e., number) of the points that can coexist for a given value of the hard core parameter. Furthermore, the gap between the true intensity and the calculated intensity of the MHCPP type II (i.e., the amount of underestimation) increases with the hard core distance and the intensity of the parent PPP. The effect of the intensity underestimation flaw of the MHCPP type II on the modeling of CSMA networks was discussed in [45], [51], where the intensity underestimation flaw was mitigated for relatively low intensities of the parent PPP. The second challenge is to obtain an expression for the distribution of the distance between a generic location and the nearest point in the HCPP. The distribution of this distance is crucial if the HCPP is used to model a cellular network because this distance refers to the distance between a user and her serving network entity. An approximate expression for this distance was derived in [41]. Another challenge is to obtain an expression for the probability generating functional in order to obtain the LT of the interference associated with a HCPP. This problem was reported in [40], [49], and approximate expressions for the LTs were derived. One interesting future direction is to address the challenges of the HCPP and extend the existing results in the literature for more accurate modeling of cellular and cognitive wireless networks.

In [89], [90], an asymptotic approach for the outage characterization of wireless networks with general node distribution and general fading was presented. This includes the PPP, HCPP, clustered PPs, and grid models as special cases, and permits arbitrary MAC schemes. However, the results are restricted to the high-SIR case. In [103], the method of factorial moment expansion [104] was used to characterize and approximate the interference in networks with general spatial distribution of nodes. The proposed model has a high potential for more accurate modeling of wireless networks and presents a clear tradeoff between the accuracy and complexity of the expressions obtained. The initiatives proposed in [89], [90], [102], [103] open the road for discovering new stochastic geometry tools for more accurate, flexible, and general modeling of wireless networks.

Another interesting future direction is to incorporate the queuing dynamics into the stochastic geometry models. Most of the work in the literature assume saturation conditions for the traffic. That is, the buffers of all network elements are always full, which might not be true and will provide a pessimistic view of the aggregate interference as well as some other performance metrics (e.g., spectrum access probability in cognitive and CSMA networks). Moreover, no insights regarding the packet delays can be obtained since the queuing dynamics are ignored. The commonly used saturation conditions were relaxed in [44], [105], [106] for ad hoc networks. However, to the best of our knowledge, there has not been any work that incorporate the queuing dynamics into the stochastic geometry models for cellular networks. [44] proposed a three-dimensional PPP to model the traffic flow for the coexisting network nodes in a CSMA network. The locations of the network nodes were modeled via a two-dimensional PPP while the traffic arrivals were modeled via a one-dimensional PPP. However, [44] only modeled the outage

probability and no insights on the packet delay performance was given. In [105], the stability and delay performances were analyzed for nodes with infinite queues in a PPP ad hoc network with one and two classes of nodes. In [106], the authors calculated bounds on the end-to-end delay, the optimum hop lengths, and the number of hops in a TDMA/ALOHA multi-hop network in the presence of a PPP field of interferers.

In the context of multi-tier cellular networks only few results are available on cognitive small cells, MIMO, optimized load balancing, mobility, and uplink network modeling. As discussed earlier, cognition provides a potential solution for dynamic spectrum allocation in multi-tier cellular networks. In [74], it was assumed that the interference seen by each antenna is independent, however, this assumption may not hold because, as shown in [35], [107], [108], the aggregate interference is correlated in time and across small spatial intervals. We would like to emphasize that in [24], [73], [74] the authors did not use any of the popular five techniques presented in Section III for the performance evaluation of the downlink coverage with MIMO transmissions. This indicates that there are opportunities for innovating techniques which facilitate the stochastic geometry modeling and get around the well-known obstacles. A mobility model that relies on stochastic geometry tools was proposed in [109] where the authors used the random waypoint mobility model to derive the cell crossing rate in cellular networks.

VII. DISCUSSIONS

Stochastic geometry is the only mathematical technique available that provides a rigorous analytical approach to the modeling, analysis, and design of HetNets and cognitive multi-tier cellular networks. While it is extremely powerful when applied to networks modeled as PPPs with Rayleigh fading, leading to short and general closed-form expressions, generalizing the network models diminishes its tractability. That said, we have seen that simple baseline stochastic geometry modeling helps understanding the effects of the fundamental design parameters on the system behavior. For instance, in [54], [55], for a network tier modeled via a PPP, it was shown that the SIR statistics do not depend on the intensity of the BSs constituting that tier. References [54], [62], [63] quantified the minimum performance gain (in terms of outage probability and average achievable rate) for different frequency reuse schemes. In [59], the effect of biasing on the achievable data rate as well as the outage probability was quantified. Spectrum sharing/partitioning was optimized in [67]–[69]. An approach towards the optimal BS deployment was proposed in [64]. The performance gain in terms of outage probability has been quantified in [77]–[80] when cognition is implemented in small cells.

The above examples show the potential of the simple baseline models and how they can be easily modified and adapted to more practical cases. Moreover, simple approximations (i.e., technique #2, technique #3) prove to be powerful yet accurate for more flexible and general modeling of wireless networks. Note that we do not have to run computationally intensive simulations to check the accuracy of the approximation techniques. Instead, the accuracy for approximation techniques can be numerically verified by comparing to the

results obtained using Plancherel-Parseval Theorem (technique #4).

Spatial averaging is argued to be another limitation for the stochastic geometry modeling. Considering only spatial averages may hide the effect of the design parameters on the uncertainties due to the spatial randomness [41], [110]. That is, the performance metrics are random variables that may vary from one location to another in the spatial domain based on the position of the tagged node w.r.t. the interference sources. Spatial averages may hide important details that impact the network performance and limit the insights that can be obtained from the spatial averaging.

For instance, with the spatial average of the outage probability, we cannot design the network such that at least 95% of the users experience an outage probability less than 1%. In [41], the authors proposed a new method based on computing the conditional performance metrics (i.e., conditioning on the number of nodes having high influence on the performance metric of interest) to analyze the effect of the design parameters on the distribution of the performance metrics.

It was shown in [41] that the sensing threshold in a CSMA network might have a significant impact on the percentiles of users experiencing negligible data rates while showing a good spatial average due to the users that have high data rates. In [110], the authors characterized the spatial distribution (instead of the spatial average) of the link outage in a PPP ad hoc network. The distribution of link outage was characterized by its moments and the Markov inequality was utilized to derive an upper bound on the spatial distribution of the link outage. The authors also used the Markov inequality to derive an upper bound on the transmission capacity, which was defined as the maximum allowable intensity of simultaneous transmissions such that a certain percentile of nodes have a success probability (the complement of outage probability) more than a predefined threshold. From the results of [41], [110] we can conclude that insights beyond spatial averages are crucial to the network performance and that stochastic geometry techniques are powerful enough to provide these insights.

VIII. CONCLUSION

Stochastic geometry modeling for multi-tier cellular and cognitive networks provides tractable and accurate expressions for the performance metrics in terms of the design parameters. A comprehensive review of the literature related to the stochastic geometry modeling of multi-tier and cognitive cellular networks has been presented. A taxonomy that reveals the popularity and applicability of different point processes and different performance evaluation techniques have also been presented. It has been shown that the baseline models developed for multi-tier cellular networks are simple, flexible and can capture many practical network properties such as frequency reuse, FFR, and cognition. The models for multi-tier cellular networks in the literature provide useful insights to the network design and have been adapted to optimize the deployment of BSs, frequency sharing/partitioning for multi-tier cellular networks, frequency reuse, transmission rate, outage probability and cognition. Looking into the literature,

we can see that technique #1 and technique #2 are the most popular performance evaluation techniques due to their simplicity and tractability. If a simple analysis is required for a network in which the channel power gain in the desired links is not exponentially distributed and also the path-loss exponent is low, then technique #3 is preferred. However, only approximate results can be obtained. On the other hand, technique #4 provides the potential to obtain the exact results via stochastic geometry modeling, however, at the expense of reduced tractability. Finally, the usage of technique #5 is limited to very special cases.

ACKNOWLEDGMENT

This work was supported in part by an IPS from Natural Sciences and Engineering Research Council of Canada (NSERC), an NSERC Strategic Grant (STPGP 430285), in part by a scholarship from TRTech, Winnipeg, Manitoba, Canada, and in part by U.S. NSF grant CCF 1216407.

REFERENCES

- [1] "More Than 50 Billion Connected Devices", Ericsson White Paper, February 2011.
- [2] K. Samdanis, T. Taleb, and S. Schmid, "Traffic Offload Enhancements for eUTRAN," *IEEE Commun. Surveys Tutorials*, vol. 14, no. 3, Third Quarter 2012, pp. 884–896.
- [3] P. Lin, J. Zhang, Y. Chen, and Q. Zhang, "Macro-Femto Heterogeneous Network Deployment and Management: From Business Models to Technical Solutions," *IEEE Wireless Commun.*, vol. 18, no. 3, pp. 64–70, June 2011.
- [4] J. Andrews, H. Claussen, M. Dohler, S. Rangan, and M. Reed, "Femtocells: Past, Present, and Future," *IEEE J. Sel. Areas Commun.*, vol. 30 no. 3, pp. 497–508, April 2012.
- [5] S. Cheng, S. Lien, F. Hu, and K. Chen, "On Exploiting Cognitive Radio to Mitigate Interference in Macro/Femto Heterogeneous Networks," *IEEE Wireless Commun.*, vol. 18, no. 3, pp. 40–47, June 2011.
- [6] N. Saquib, E. Hossain, L. B. Le, and D. I. Kim, "Interference Management in OFDMA Femtocell Networks: Issues and Approaches," *IEEE Wireless Commun.*, vol. 19, no. 3, pp. 86–95, June 2012.
- [7] D. Perez, I. Guvenc, G. de la Roche, M. Kountouris, T. Quek, and J. Zhang, "Enhanced Inter-Cell Interference Coordination Challenges in Heterogeneous Networks," *IEEE Wireless Commun.*, vol. 18, no. 3, pp. 22–30, June 2011.
- [8] K. Gilhousen, I. Jacobs, R. Padovani, A. J. Viterbi, L. Weaver, and C. Wheatley, "On the Capacity of a Cellular CDMA System," *IEEE Trans. Veh. Technol.*, vol. 40, no. 2, pp. 303–312, May 1991.
- [9] J. Xu, J. Zhang, and J. G. Andrews, "On the Accuracy of the Wyner Model in Cellular Networks," *IEEE Trans. Wireless Commun.*, vol. 10, no. 9, pp. 3098–3109, September 2011.
- [10] M. Haenggi, *Stochastic Geometry for Wireless Networks*. Cambridge University Press, 2012.
- [11] M. Haenggi, J. G. Andrews, F. Baccelli, O. Dousse, and M. Franceschetti, "Stochastic Geometry and Random Graphs for the Analysis and Design of Wireless Networks," *IEEE J. Sel. Areas Commun.*, vol. 27, no. 7, pp. 1029–1046, September 2009.
- [12] P. Cardieri, "Modeling Interference in Wireless Ad hoc Networks," *IEEE Commun. Surveys Tutorials*, vol. 12, no. 4, pp. 551–572, Fourth Quarter 2010.
- [13] M. Haenggi and R. Ganti, *Interference in Large Wireless Networks*, in *Foundations and Trends in Networking*, NOW Publishers, 2008, vol. 3, no. 2, pp. 127–248.
- [14] S. Weber and J. G. Andrews, *Transmission Capacity of Wireless Networks in Foundations and Trends in Networking*, NOW Publishers, February 2012.
- [15] F. Baccelli and B. Blaszczyzyn, *Stochastic Geometry and Wireless Networks in Foundations and Trends in Networking*, Volume 1, NOW Publishers, 2009.
- [16] F. Baccelli and B. Blaszczyzyn, *Stochastic Geometry and Wireless Networks in Foundations and Trends in Networking*, Volume 2, NOW Publishers, 2009.
- [17] L. Kleinrock and J. A. Silvester, "Optimum Transmission Radii for Packet Radio Networks or Why Six is a Magic Number," in *Conference Record: National Telecommunication Conference*, December 1978, pp. 4.3.1–4.3.5.
- [18] T. Hou and V. Li, "Transmission Range Control in Multihop Packet Radio Networks," *IEEE Trans. Commun.*, vol. 34, no. 1, pp. 38–44, January 1986.
- [19] R. Mathar and J. Mattfeldt, "On the Distribution of Cumulated Interference Power in Rayleigh Fading Channels," *Wireless Networks*, vol. 1, pp. 31–36, February 1995.
- [20] S. Weber, J. G. Andrews and N. Jindal, "The Effect of Fading, Channel Inversion and Threshold Scheduling on Ad Hoc Networks," *IEEE Trans. Inf. Theory*, vol. 53, no. 11, pp. 4127–4149, November 2007.
- [21] S. Weber, X. Yang, J. G. Andrews, and G. de Veciana, "Transmission Capacity of Wireless Ad hoc Networks with Outage Constraints," *IEEE Trans. Inf. Theory*, vol. 51, no. 12, pp. 4091–4102, December 2005.
- [22] S. Weber, J. Andrews, X. Yang, and G. de Veciana, "Transmission Capacity of Wireless Ad Hoc Networks with Successive Interference Cancellation," *IEEE Trans. Inf. Theory*, vol. 53, no. 8, pp. 2799–2814, August 2007.
- [23] N. Jindal, S. Weber and J. G. Andrews, "Fractional Power Control for Decentralized Wireless Networks," *IEEE Trans. Wireless Commun.*, vol. 7, no. 12, pp. 5482–5492, December 2008.
- [24] A. M. Hunter, J. G. Andrews and S. P. Weber, "Transmission Capacity of Ad Hoc Networks with Spatial Diversity," *IEEE Trans. Wireless Commun.*, vol. 7, no. 12, pp. 5058–71, December 2008.
- [25] J. Venkataraman, M. Haenggi, and O. Collins, "Shot Noise Models for Outage and Throughput Analyses in Wireless Ad hoc Networks," in *Proc. of IEEE Military Commun. Conf. (MILCOM'06)*, Washington, DC, USA, October 2006.
- [26] S. Weber, J. G. Andrews, and N. Jindal, "An Overview of the Transmission Capacity of Wireless Networks," *IEEE Trans. Commun.*, vol. 58, no. 12, December 2010.
- [27] J. Venkataraman, M. Haenggi, and O. Collins, "Shot Noise Models for the Dual Problems of Cooperative Coverage and Outage in Random Networks," in *Proc. 44th Annual Allerton Conf. Commun., Control, and Comput. (Allerton'06)*, Monticello, IL, USA, September 2006.
- [28] E. S. Sousa, "Optimum Transmission Range in a Direct-sequence Spread Spectrum Multihop Packet Radio Network," *IEEE J. Sel. Areas Commun.*, vol. 8, no. 5, pp. 762–771, 1990.
- [29] M. Souryal, B. Vojcic and R. Pickholtz, "Ad hoc, Multihop CDMA Networks with Route Diversity in a Rayleigh Fading Channel," in *Proc. IEEE Military Commun. Conf. (MILCOM'01)* pp. 1003–1007, October 2001.
- [30] H. Inaltekin, S. B. Wicker, M. Chiang, and H. V. Poor, "On Unbounded Path-loss Models: Effects of Singularity on Wireless Network Performance," *IEEE J. Sel. Areas Commun.*, pp. 1078–1092, 2009.
- [31] M. Z. Win, P. C. Pinto, and L. A. Shepp, "A Mathematical Theory of Network Interference and Its Applications," in *Proc. IEEE*, vol. 97, no. 2, pp. 205–230, 2009.
- [32] F. Baccelli, B. Blaszczyzyn, and P. Mühlethaler, "Stochastic Analysis of Spatial and Opportunistic ALOHA," *IEEE J. Sel. Areas Commun.*, vol. 27, no. 7, pp. 1105–1119, September 2009.
- [33] X. Zhang and M. Haenggi, "Random Power Control in Poisson Networks," *IEEE Trans. Commun.*, vol. 60, pp. 2602–2611, Sept. 2012.
- [34] X. Zhang and M. Haenggi, "Delay-optimal Power Control Policies," *IEEE Trans. Wireless Commun.*, vol. 11, pp. 3518–3527, Oct. 2012.
- [35] Z. Gong and M. Haenggi, "Interference and Outage in Mobile Random Networks: Expectation, Distribution, and Correlation," *IEEE Trans. Mobile Computing*, 2012. Accepted.
- [36] M. Haenggi, "On Distances in Uniformly Random Networks," *IEEE Trans. Inf. Theory*, vol. 51, pp. 3584–3586, October 2005.
- [37] S. Srinivasa and M. Haenggi, "Modeling Interference in Finite Uniformly Random Networks," in *International Workshop on Information Theory for Sensor Networks (WITS 2007)*, Santa Fe, NM, June 2007.
- [38] S. Srinivasa and M. Haenggi, "Distance Distributions in Finite Uniformly Random Networks: Theory and Applications," *IEEE Trans. Veh. Technol.*, vol. 59, pp. 940–949, February 2010.
- [39] R. K. Ganti and M. Haenggi, "Interference and Outage in Clustered Wireless Ad Hoc Networks," *IEEE Trans. Inf. Theory*, vol. 55, pp. 4067–4086, September 2009.
- [40] H. Nguyen, F. Baccelli, and D. Kofman, "A Stochastic Geometry Analysis of Dense IEEE 802.11 Networks," in *Proc. 26th IEEE International Conference on Computer Communications (INFOCOM'07)*, May 2007, pp. 1199–1207.
- [41] G. Alfano, M. Garetto, and E. Leonardi, "New Insights into the Stochastic Geometry Analysis of Dense CSMA Networks," in *Proc.*

- 30th Annual IEEE International Conference on Computer Communications (INFOCOM'11), April 2011, pp. 2642–2650.
- [42] Y. Kim, F. Baccelli, and G. de Veciana, "Spatial Reuse and Fairness of Mobile Ad-hoc Networks with Channel-aware CSMA Protocols," in *Proc. 17th Workshop on Spatial Stochastic Models for Wireless Networks*, May 2011.
- [43] A. Hasan and J. G. Andrews, "The Guard Zone in Wireless Ad hoc Networks," *IEEE Trans. Wireless Commun.*, vol. 4, no. 3, pp. 897–906, March 2007.
- [44] M. Kaynia, N. Jindal, and G. Oien, "Improving the Performance of Wireless Ad hoc Networks through MAC Layer Design," *IEEE Trans. Wireless Commun.*, vol. 10, no. 1, pp. 240–252, January 2011.
- [45] H. ElSawy and E. Hossain, "A Modified Hard Core Point Process for Analysis of Random CSMA Wireless Networks in General Fading Environments," *IEEE Trans. Commun.*, accepted.
- [46] H. ElSawy, E. Hossain, and S. Camorlinga, "Spectrum-efficient Multi-channel Design for Coexisting IEEE 802.15.4 Networks: A Stochastic Geometry Approach," submitted to the *IEEE Trans. Mobile Computing*.
- [47] H. ElSawy, E. Hossain, and S. Camorlinga, "Multi-channel Design for Random CSMA Wireless Networks: Stochastic Geometry Approach," in *Proc. IEEE Int. Conference on Communications (ICC'13)*, Budapest, Hungary, 9-13 June, 2013.
- [48] P. Mühlethaler and A. Najid, "Throughput Optimization of a Multihop CSMA Mobile Ad hoc Network," INRIA, Research Report 4928, September 2003.
- [49] M. Haenggi, "Mean Interference in Hard-core Wireless Networks," *IEEE Communications Letters*, vol. 15, pp. 792–794, August 2011.
- [50] H. ElSawy and E. Hossain, "Modeling Random CSMA Wireless Networks in General Fading Environments," in *Proc. IEEE Int. Conf. on Communications (ICC 2012)*, Ottawa, Canada, 10-15 June 2012.
- [51] H. ElSawy, E. Hossain, and S. Camorlinga, "Characterizing Random CSMA Wireless Networks: A Stochastic Geometry Approach," in *Proc. IEEE Int. Conf. on Communications (ICC 2012)*, Ottawa, Canada, 10-15 June 2012.
- [52] F. Baccelli, M. Klein, M. Lebourges, and S. Zuyev, "Stochastic Geometry and Architecture of Communication Networks," *J. Telecommunication Systems*, vol. 7, no. 1, pp. 209–227, 1997.
- [53] T. X. Brown, "Cellular Performance Bounds via Shotgun Cellular Systems," *IEEE J. Sel. Areas Commun.*, vol. 18, no. 11, Nov. 2000, pp. 2443–2455.
- [54] J. Andrews, F. Baccelli, and R. Ganti, "A Tractable Approach to Coverage and Rate in Cellular Networks," *IEEE Trans. Commun.*, vol. 59, no. 11, pp. 3122–3134 November 2011.
- [55] H. Dhillon, R. Ganti, F. Baccelli, and J. Andrews, "Modeling and Analysis of K-Tier Downlink Heterogeneous Cellular Networks," *IEEE J. Sel. Areas Commun.*, vol. 30, no. 3, pp. 550–560, April 2012.
- [56] S. Singh, H. S. Dhillon, and J. G. Andrews, "Offloading in Heterogeneous Networks: Modeling, Analysis, and Design Insights," *IEEE Trans. Wireless Commun.*, accepted.
- [57] H. Dhillon, T. Novlan, J. Andrews, "Coverage Probability of Uplink Cellular Networks," in *Proc. IEEE Global Communications Conference (GLOBECOM 2012)*, 3-7 December, Anaheim, CA, USA, 2012.
- [58] H. S. Dhillon, R. K. Ganti and J. G. Andrews, "Load-Aware Modeling and Analysis of Heterogeneous Cellular Networks," *IEEE Trans. Wireless Commun.*, Vol. 12, No. 4, April 2013.
- [59] H. Jo, Y. Sang, P. Xia, and J. Andrews, "Outage Probability for Heterogeneous Cellular Networks with Biased Cell Association," in *Proc. IEEE Global Communications Conference (GLOBECOM 2011)*, 5-9 December, Houston, TX, USA, 2011.
- [60] H. Jo, Y. Sang, P. Xia, and J. Andrews, "Heterogeneous Cellular Networks With Flexible Cell Association: A Comprehensive Downlink SINR Analysis," *IEEE Trans. Wireless Commun.*, vol. 11, no. 9, pp. 3484–3495, October 2012.
- [61] H. ElSawy, E. Hossain, and S. Camorlinga, "Offloading Techniques in Two-tier Femtocell Networks," in *Proc. IEEE Int. Conference on Communications (ICC'13)*, Budapest, Hungary, 9-13 June 2013.
- [62] T. Novlan, R. Ganti, A. Ghosh, and J. Andrews, "Analytical Evaluation of Fractional Frequency Reuse for OFDMA Cellular Networks," *IEEE Trans. Wireless Commun.*, vol. 10, no. 12, pp. 4294–4305, December 2011.
- [63] T. Novlan, R. Ganti, A. Ghosh, and J. Andrews, "Analytical Evaluation of Fractional Frequency Reuse for Heterogeneous Cellular Networks," *IEEE Trans. Commun.*, vol. 60, no. 7, pp. 2029–2039, July 2012.
- [64] D. Cao, S. Zhou, and Z. Niu, "Optimal Base Station Density for Energy-efficient Heterogeneous Cellular Networks," in *Proc. IEEE Int. Conf. on Communications (ICC 2012)*, Ottawa, Canada, 10-15 June 2012.
- [65] Y. Zhong and W. Zhang, "Downlink Analysis of Multi-channel Hybrid Access Two-tier Networks," in *Proc. IEEE Int. Conf. on Communications (ICC 2012)*, Ottawa, Canada, 10-15 June 2012.
- [66] S. Mukherjee, "Distribution of Downlink SINR in Heterogeneous Cellular Networks," *IEEE J. Sel. Areas Commun.*, vol. 30, no. 3, pp. 575–585, April 2012.
- [67] V. Chandrasekhar and J. Andrews, "Spectrum Allocation in Tiered Cellular Networks," *IEEE Trans. Commun.*, vol. 57, no. 10, pp. 3059–3068, October 2009.
- [68] W. Cheung, T. Quek, and M. Kountouris, "Throughput Optimization, Spectrum Allocation, and Access Control in Two-tier Femtocell Networks," *IEEE J. Sel. Areas Commun.*, vol. 30, no. 3, pp. 561–574, April 2012.
- [69] K. Huang, V. Lau, and Y. Chen, "Spectrum Sharing between Cellular and Mobile Ad hoc Networks: Transmission-capacity Tradeoff," *IEEE J. Sel. Areas Commun.*, vol. 27, no. 7, pp. 1256–1266, September 2009.
- [70] V. Chandrasekhar and J. Andrews, "Uplink Capacity and Interference Avoidance for Two-tier Femtocell Networks," *IEEE Trans. Wireless Commun.*, vol. 8, no. 7, pp. 3498–3509, July 2009.
- [71] P. Pinto, A. Giorgetti, M. Win, and M. Chiani, "A Stochastic Geometry Approach to Coexistence in Heterogeneous Wireless Networks," *IEEE J. Sel. Areas Commun.*, vol. 27, no. 7, pp. 1268–1282, September 2009.
- [72] A. Guidotti, M. Di Renzo, G. Corazza, and F. Santucci, "Simplified Expression of the Average Rate of Cellular Networks Using Stochastic Geometry," in *Proc. IEEE Int. Conf. on Communications (ICC 2012)*, Ottawa, Canada, 10-15 June 2012.
- [73] R. W. Heath, M. Kountouris, "Modeling heterogeneous network interference," in *Proc. Information Theory and Applications Workshop (ITA)*, pp.17–22, 5-10 Feb. 2012
- [74] H. Dhillon, M. Kountouris, J. Andrews, "Downlink Coverage Probability in MIMO HetNets," in *Proc. 46th Annual Asilomar Conference on Signals, Systems, and Computers*, 4-7 November, Pacific Grove, CA, USA, 2012.
- [75] R. W. Heath, M. Kountouris, and T. Bai, "Modeling Heterogeneous Network Interference With Using Poisson Point Processes," submitted to *IEEE Trans. Signal Process.*, July 2012. Available Online: (<http://arxiv.org/abs/1207.2041>).
- [76] C. Lima, M. Bennis, and M. Latva-aho, "Coordination Mechanisms for Self-Organizing Femtocells in Two-Tier Coexistence Scenarios," *IEEE Trans. Wireless Commun.*, vol. 11, no. 6, pp. 2212–2223, June 2012.
- [77] H. ElSawy and E. Hossain, "Two-Tier HetNets with Cognitive Femtocells: Downlink Performance Modeling and Analysis in a Multi-Channel Environment," *IEEE Trans. Mobile Computing*, accepted.
- [78] H. ElSawy and E. Hossain, "On Cognitive Small Cells in Two-tier Heterogeneous Networks," in *Proc. 9th Workshop on Spatial Stochastic Models for Wireless Networks (SpaSWiN 2013)*, Tsukuba Science City, Japan, May 13-17, 2013.
- [79] H. ElSawy, E. Hossain, and D. I. Kim, "HetNets with Cognitive Small Cells: User Offloading and Distributed Channel Allocation Techniques," *IEEE Commun. Mag.*, Special Issue on "Heterogeneous and Small Cell Networks (HetSNets)", May 2013.
- [80] H. ElSawy and E. Hossain, "Channel Assignment and Opportunistic Spectrum Access in Two-tier Cellular Networks with Cognitive Small Cells," submitted to *IEEE Global Communications Conference (GLOBECOM 2013)*, Atlanta, GA, USA, 9-13 December 2013.
- [81] M. Khoshkholgh, K. Navaie, and H. Yanikomeroglu, "Outage Performance of the Primary Service in Spectrum Sharing Networks," *IEEE Trans. Mobile Computing*, Accepted, 2012.
- [82] A. Ghasemi and E. Sousa, "Interference Aggregation in Spectrum Sensing Cognitive Wireless Networks," *IEEE J. Sel. Topics Signal Process.*, vol. 2, no. 1, pp. 41–56, February 2008.
- [83] C.-H. Lee and M. Haenggi, "Interference and Outage in Poisson Cognitive Networks," *IEEE Trans. Wireless Commun.*, vol. 11, pp. 1392–1401, April 2012.
- [84] A. Rabbachin, T. Q. S. Quek, H. Shin, and M. Z. Win, "Cognitive Network Interference," *IEEE J. Sel. Areas Commun.*, vol. 29, no. 2, pp. 480–493, February 2011.
- [85] T. Nguyen and F. Baccelli, "A Probabilistic Model of Carrier Sensing Based Cognitive Radio," in *Proc. IEEE Symposium on New Frontiers in Dynamic Spectrum Access Networks*, pp. 1–12, April 2010.
- [86] T. Nguyen and F. Baccelli, "Stochastic Modeling of Carrier Sensing Based Cognitive Radio Networks," in *Proc. 8th International Symposium on Modeling and Optimization in Mobile, Ad Hoc and Wireless Networks (WiOpt)*, pp. 472–480, June 2010.
- [87] J. Møller, M. L. Huber, and R. L. Wolpert, "Perfect Simulation and Moment Properties for the Matérn Type III Process," *Stochastic Processes and Their Applications*, vol. 120, no. 11, November 2010, pp. 2142–2158.

- [88] M. L. Huber and R. L. Wolpert, "Likelihood Based Inference for Matérn Type III Repulsive Point Processes," *Advances in Applied Probability*, vol. 41, no. 4, 2009, pp. 958–977.
- [89] R. K. Ganti, J. G. Andrews, and M. Haenggi, "High-SIR Transmission Capacity of Wireless Networks with General Fading and Node Distribution," *IEEE Trans. Inf. Theory*, vol. 57, pp. 3100–3116, May 2011.
- [90] R. Giacomelli, R. K. Ganti, and M. Haenggi, "Outage Probability of General Ad hoc Networks in the High-reliability Regime," *IEEE/ACM Trans. Netw.*, vol. 19, pp. 1151–1163, August 2011.
- [91] P. Brémaud, *Mathematical Principles of Signal Processing: Fourier and Wavelet Analysis*. Springer, 2002.
- [92] A. Guo and M. Haenggi, "Spatial Stochastic Models and Metrics for the Structure of Base Stations in Cellular Networks," submitted to *IEEE Trans. Wireless Commun.*, 2013. Available Online: <http://www.nd.edu/~mhaenggi/pubs/twc13b.pdf>.
- [93] B. Blaszczyzyn, M. K. Karray, and H.-P. Keeler, "Using Poisson Processes to Model Lattice Cellular Networks," in *Proc. 32th Annual IEEE International Conference on Computer Communications (INFOCOM'13)*, Turin, Italy, April 14–19 2013.
- [94] A. Okabe, B. Boots, and K. Sugihara, *Spatial Tessellations: Concepts and Applications of Voronoi Diagrams*. John Wiley, 1992.
- [95] K. Hamdi, "A Useful Lemma for Capacity Analysis of Fading Interference Channels," *IEEE Trans. Commun.*, vol. 58, no. 2, pp. 411–416, February 2010.
- [96] N. Saquib, E. Hossain, and D. I. Kim, "Fractional Frequency Reuse for Interference Management in LTE-Advanced HetNets," *IEEE Wireless Commun.*, to appear.
- [97] P. Mitran and C. Rosenberg, "On Fractional Frequency Reuse in Imperfect Cellular Grids," in *Proc. IEEE Wireless Communications and Networking Conference (WCNC 2012)*, Paris, France, pp. 2967–2972, April 2012.
- [98] R. Trestian, O. Ormond, and G. Muntean, "Game Theory-Based Network Selection: Solutions and Challenges," *IEEE Commun. Surveys Tutorials*, vol. 14, no. 4, pp. 1212–1231, Fourth Quarter 2012.
- [99] 3GPP TR 36.942, Radio Frequency (RF) system scenarios (Release 10), Dec. 2010.
- [100] 3GPP TSG RAN WG1, R1-101506, Importance of serving cell selection in heterogeneous networks, Qualcomm Incorporated, San Francisco, Feb. 2010.
- [101] G. de la Roche, A. Valcarce, D. Lopez-Perez, and J. Zhang, "Access Control Mechanisms for Femtocells," *IEEE Communications Magazine*, vol. 48, no. 1, pp. 33–39, January, 2010
- [102] D. Taylor, H. Dhillon, T. Novlan, and J. Andrews, "Pairwise Interaction Processes for Modeling Cellular Network Topology," in *Proc. IEEE Global Communications Conference (Globecom 2012)*, 3–7 December, Anaheim, CA, USA, 2012.
- [103] R. Ganti, F. Baccelli, and J. Andrews, "Series Expansion for Interference in Wireless Networks," *IEEE Trans. Inf. Theory*, vol. 58, no. 4, pp. 2194–2205, April 2012.
- [104] B. Blaszczyzyn, "Factorial Moment Expansion for Stochastic Systems," *Stochastic Processes and Their Applications*, vol. 56, no. 2, pp. 321–335, 1995.
- [105] K. Stamatiou and M. Haenggi, "Random-Access Poisson Networks: Stability and Delay," *IEEE Commun. Lett.*, vol. 14, pp. 1035–1037, November 2010.
- [106] K. Stamatiou and M. Haenggi, "Delay Characterization of Multihop Transmission in a Poisson Field of Interference," *IEEE/ACM Trans. Netw.*, 2011. Submitted, available at (<http://www.nd.edu/~mhaenggi/pubs/ton11b.pdf>).
- [107] M. Haenggi, "Diversity Loss due to Interference Correlation," *IEEE Commun. Lett.*, vol. 16, pp. 1600–1603, October 2012.
- [108] R. K. Ganti and M. Haenggi, "Spatial and Temporal Correlation of the Interference in ALOHA Ad Hoc Networks," *IEEE Commun. Lett.*, vol. 13, pp. 631–633, September 2009.
- [109] X. Lin, R. Ganti, P. Fleming, and J. Andrews, "Fundamentals of Mobility in Cellular Networks: Modeling and Analysis," in *Proc. of IEEE Global Communications Conference (Globecom 2012)*, 3–7 December, Anaheim, CA, USA, 2012.
- [110] R. K. Ganti and J. G. Andrews, "Correlation of Link Outages in Low-mobility Spatial Wireless Networks," in *Proc. 2010 Forty Fourth Asilomar Conference on Signals, Systems and Computers (ASILOMAR)*, pp. 312–316, 7–10 November 2010.



Hesham ElSawy received his B.Sc and M.Sc both in electrical engineering from Assiut University, Assiut, Egypt, and Arab Academy for Science and Technology, Cairo, Egypt, in 2006 and 2009, respectively. Currently, he is a Ph.D. candidate in the department of Electrical and Computer Engineering, University of Manitoba, Canada. During the period of 2006 to 2010, he worked at the National Telecommunication Institute, Egypt, where he conducted professional training both at the national and international levels, as well as research on network planning. Since 2010, he has been with TRTech, Winnipeg, Canada, as a student researcher. For his academic excellence, Hesham has received several academic awards including the NSERC Industrial Postgraduate Scholarship during the period of 2010–2013, and the TRTech graduate students fellowship in the period of 2010–2014. Hesham's research interests include statistical modeling of wireless networks, stochastic geometry and queuing analysis for wireless communication networks.



Ekram Hossain is a Professor in the Department of Electrical and Computer Engineering at University of Manitoba, Winnipeg, Canada. He received his Ph.D. in Electrical Engineering from University of Victoria, Canada, in 2001. Dr. Hossain's current research interests include design, analysis, and optimization of wireless/mobile communications networks, cognitive radio systems, and network economics. He has authored/edited several books in these areas (<http://www.ee.umanitoba.ca/~ekram>).

Dr. Hossain serves as the Editor-in-Chief for the IEEE Communications Surveys and Tutorials (for the term 2012–2013), an Editor for the *IEEE J. Sel. Areas Commun. - Cognitive Radio Series* and *IEEE Wireless Communications*. Also, he serves on the IEEE Press Editorial Board (for the term 2013–2015). Previously, he served as the Area Editor for the *IEEE Trans. Wireless Commun.* in the area of "Resource Management and Multiple Access" from 2009–2011 and an Editor for the *IEEE Trans. Mobile Computing* from 2007–2012. Dr. Hossain has won several research awards including the University of Manitoba Merit Award in 2010 (for Research and Scholarly Activities), the 2011 IEEE Communications Society Fred Ellersick Prize Paper Award, and the IEEE Wireless Communications and Networking Conference 2012 (WCNC'12) Best Paper Award. He is a Distinguished Lecturer of the IEEE Communications Society for the term 2012–2013. Dr. Hossain is a registered Professional Engineer in the province of Manitoba, Canada.



Martin Haenggi is a Professor of Electrical Engineering and a Concurrent Professor of Applied and Computational Mathematics and Statistics at the University of Notre Dame, Indiana, USA. He received the Dipl.-Ing. (M.Sc.) and Dr.sc.techn. (Ph.D.) degrees in electrical engineering from the Swiss Federal Institute of Technology in Zurich (ETH) in 1995 and 1999, respectively. After a postdoctoral year at the University of California in Berkeley, he joined the University of Notre Dame in 2001. In 2007-08, he spent a Sabbatical Year at the

University of California at San Diego (UCSD). For both his M.Sc. and his Ph.D. theses, he was awarded the ETH medal, and he received a CAREER award from the U.S. National Science Foundation in 2005 and the 2010 IEEE Communications Society Best Tutorial Paper award. He served as a member of the Editorial Board of the Elsevier Journal of Ad Hoc Networks from

2005-08, as a Guest Editor for the *IEEE J. Sel. Areas Commun.* in 2008-09, as an Associate Editor for the *IEEE Trans. Mobile Computing* from 2008-11 and for the *ACM Transactions on Sensor Networks* from 2009-11, and as a Distinguished Lecturer for the IEEE Circuits and Systems Society in 2005-06. He also served as a TPC Co-chair of the Communication Theory Symposium of the 2012 IEEE International Conference on Communications (ICC12), and as a General Co-chair of the 2009 International Workshop on Spatial Stochastic Models for Wireless Networks and the 2012 DIMACS Workshop on Connectivity and Resilience of Large-Scale Networks. Presently he is a Steering Committee Member of the *IEEE Trans. Mobile Computing*. He is a co-author of the monograph "Interference in Large Wireless Networks" (NOW Publishers, 2009) and the author of the textbook *Stochastic Geometry for Wireless Networks* (Cambridge University Press, 2012). His scientific interests include networking and wireless communications, with an emphasis on ad hoc, cognitive, cellular, sensor, and mesh networks.